energies

MDPI

Review

Generative Design of Concentrated Solar Thermal Tower Receivers—State of the Art and Trends

Jorge Moreno García-Moreno and Kypros Milidonis *

Energy, Environment and Water Research Center (EEWRC), The Cyprus Institute, Nicosia 2121, Cyprus; j.moreno@cyi.ac.cy

* Correspondence: k.milidonis@cyi.ac.cy; Tel.: +357-22-208-708

Abstract

The rapid advances in artificial intelligence (AI) and high-performance computing (HPC) are transforming the landscape of engineering design, and the concentrated solar power (CSP) tower sector is no exception. As these technologies increasingly penetrate the energy domain, they bring new capabilities for addressing the complex, multi-variable nature of receiver design and optimisation. This review explores the application of AI-driven generative design techniques in the context of CSP tower receivers, with a particular focus on the use of metaheuristic algorithms and machine learning models. A structured classification is presented, highlighting the most commonly employed methods, such as Genetic Algorithms (GAs), Particle Swarm Optimisation (PSO), and Artificial Neural Networks (ANNs), and mapping them to specific receiver types: cavity, external, and volumetric. GAs are found to dominate multi-objective optimisation tasks, especially those involving trade-offs between thermal efficiency and heat flux uniformity, while ANNs offer strong potential as surrogate models for accelerating design iterations. The review also identifies existing gaps in the literature and outlines future opportunities, including the integration of high-fidelity simulations and experimental validation into AI design workflows. These insights demonstrate the growing relevance and impact of AI in advancing the next generation of high-performance CSP receiver systems.

Keywords: generative design; artificial intelligence; concentrating solar thermal; solar tower receiver; metaheuristic algorithms; Artificial Neural Networks; thermal receiver optimisation

check for updates

Academic Editor: Shin Young Jeong

Received: 9 July 2025
Revised: 30 October 2025
Accepted: 5 November 2025
Published: 8 November 2025

Citation: Moreno García-Moreno, J.; Milidonis, K. Generative Design of Concentrated Solar Thermal Tower Receivers—State of the Art and Trends. *Energies* **2025**, *18*, 5890. https://doi.org/10.3390/en18225890

Copyright: © 2025 by the authors. Licensee MDPI, Basel, Switzerland. This article is an open access article distributed under the terms and conditions of the Creative Commons Attribution (CC BY) license (https://creativecommons.org/licenses/by/4.0/).

1. Introduction

Generative design is considered the design process that involves using algorithms and computational methods to explore a range of possible solutions and design variants for a specific problem, within a design space that is governed by a set of constraints and objective functions/goals [1]. For a given problem, the process usually involves adopting a computer-driven design workflow that generates multiple design iterations that meet the design goals and satisfy the set design criteria. The workflow often employs tools and resources such as optimisation algorithms, parametric modelling software, experimental and/or simulation data, etc., that work interoperably to explore a wide range of design possibilities, often creating complex and innovative solutions that may not have been immediately apparent through traditional design optimisation methods.

In recent decades, the immense technological boom and advances in the field of artificial intelligence (AI) have unleashed tremendous capabilities, revolutionising the

generative design process [2]. Integrating computer-based intelligence through AI algorithms in the generative design workflow tremendously augmented the design process through intelligent decision-making procedures, enhanced problem-solving capabilities, adaptive and data-driven self-learning approaches, etc, making the potential application of generative design approaches virtually limitless in scope. On top of this, the nearly infinite computing resources that are nowadays highly accessible through high-performance computing (HPC) facilities play a crucial role in supporting the computational demands of the AI-driven generative design workflow. Combining these technologies enables more advanced, efficient, powerful, and scalable solutions for addressing highly complex and multidimensional design challenges across various and diverse domains.

Inevitably, given the potential of generative design, such approaches have been widely used by designers and engineers in multiple and diverse industries over a wide range of applications, revolutionising the engineering design process by converging to optimised designs that improve the efficiency of systems, reducing costs and material consumption, and, overall, enhancing the performance of engineering systems. Typical applications include the design of parts for the aviation industry [3,4], the design of parts or systems for the aerospace industry [5], the design of automotive components [6], the design of biomedical devices [7], and architectural design [8], to name but a few. In the renewable energy industry, generative design approaches have been mainly applied to the optimisation of the layout of photovoltaic modules to maximise the energy output and minimise space requirements [9], and to the design of more efficient wind turbine components [10] and blade airfoil shapes [11].

In the concentrated solar thermal (CST) technology sector, applications of generative design approaches have been found particularly useful for heliostat field topology optimisation studies (i.e., Noone et al. [12]), weather prediction (i.e., [13]), heat transfer fluid-dynamics evaluation (i.e., [14]), thermal and mechanical analysis (i.e., [15,16]), thermal energy storage prediction, control, and optimisation (i.e [17]), heliostat aiming strategy studies (i.e., [18]), the hybridridisation of CST power plants (i.e [19]), energy production prediction (i.e., [20]), and relevant techno-economical analyses (i.e., [21]). A particular application of generative design that has gained significant attention in the CST sector is the optimisation of thermal receiver geometry. This is because the receiver's design is crucial for maximising heat absorption, minimising thermal losses, and ensuring structural integrity under extreme operating conditions. Traditionally, receiver design has relied on conventional engineering methods, which often involve iterative simulations, empirical correlations, and/or parametric modelling. While these methods provide valuable insights and lead to functional receiver designs, they are time-consuming, constrained by predefined assumptions, and may not fully exploit the complex interplay between optical, thermal, and mechanical factors. In contrast, AI-driven generative design, through the use of computational algorithms and multi-objective optimisation, enables the discovery of innovative receiver configurations that enhance efficiency and performance. This approach allows for the exploration of complex, non-intuitive geometries that conventional methods might often overlook.

The rapid advancement of artificial intelligence (AI) techniques and their growing application in energy systems over the past decade have created new opportunities for optimising the design and performance of concentrated solar thermal (CST) technologies. In particular, generative design methods, enabled by algorithms such as Genetic Algorithms (GA), Particle Swarm Optimisation (PSO), and Artificial Neural Networks (ANNs), have shown significant potential in enhancing the thermal and geometric performance of CST tower receivers. However, despite this growing interest, there remains a notable gap in the systematic literature specifically addressing how these AI-based techniques are applied

to CST receiver design. While previous reviews have examined CST technologies more broadly, or optimisation methods in general, none have provided a structured, comparative analysis focused on the application of AI-driven generative design to CST receiver geometries. To the best of our knowledge, this is the first review to classify AI techniques by receiver type (cavity, external, volumetric) and map each method to its corresponding optimisation application. This makes the present work both timely and necessary, offering a foundation for future research at the intersection of AI, generative design, and solar thermal engineering. Firstly, Section 2 explains the process followed for the literature research. In Section 3, a brief description of the typical layout and operation of a CST tower system is provided, while in Section 4, a brief overview of the three most commonly used types of receiver systems in such plants is presented. Section 5 provides a general overview of the AI techniques that are mostly employed in the literature for the generative design of receivers, providing a short explanation of their operational characteristics. This is followed by an exhaustive and comprehensive review on the application of such AI techniques for the generative design optimisation of receiver geometries (Section 6). In Section 7, a critical discussion is performed highlighting the observed advantages and disadvantages of each AI technique, and finally, Section 8 presents the conclusions of the review.

2. Literature Search Methodology

To ensure the systematic and comprehensive nature of this review, a structured literature search was conducted using multiple academic databases, including Web of Science, Scopus, and ScienceDirect. The objective was to identify peer-reviewed studies that apply AI and generative design techniques to the optimisation of concentrated solar thermal (CST) tower receivers.

The search was performed using a range of keyword combinations and Boolean operators, designed to broadly capture the intersection of AI-driven optimisation and CST receiver technologies. These included phrases such as “generative design AND solar receiver,” “AI optimisation AND CST,” “artificial intelligence AND concentrated solar power,” “metaheuristic algorithms AND solar thermal,” and specific algorithm-focused terms like “receiver optimisation AND genetic algorithm,” “PSO,” “ANN,” or “NSGA-II.” To expand the scope and include cross-disciplinary contributions, additional combinations were considered, such as “generative design AND radiant enclosures,” “AI-based optimisation AND solar collectors,” and “multi-objective optimisation AND thermal receivers.” These search strategies were aimed at capturing both foundational work and the most recent advances in the field.

The literature search was limited to English-language documents, including peer-reviewed journal articles and conference proceedings. No specific publication time frame was imposed in order to provide an inclusive and complete overview of the research landscape. This approach ensured that both early contributions and recent developments in CST receiver design could be captured and analysed. Nonetheless, it was observed that the majority of relevant studies were published in the last decade, reflecting the rapid rise of interest and activity in this area.

The initial search identified over 300 publications. After applying relevance screening based on titles, abstracts, and full-text reviews, a total of 65 studies were selected for in-depth analysis. These studies were included based on their clear focus on AI-based or generative optimisation of CST receiver geometries—particularly cavity, external, and volumetric types. Publications that lacked direct relevance to receiver design or that focused on unrelated solar technologies (e.g., parabolic troughs or PV systems) were excluded from the review.

This systematic approach ensures that the present review provides a comprehensive, transparent, and well-structured synthesis of the current state of research in generative design for CST tower receivers, while also highlighting emerging trends and future research opportunities.

3. Concentrated Solar Thermal Tower Systems

A typical concentrated solar thermal (CST) tower system, also known as a solar power tower, solar tower, or central receiver system, is a solar thermal power technology that utilises an array of two-axis sun-tracking mirrors, called heliostats, to focus direct normal irradiance (DNI) onto a central receiver located atop a tower (see Figure 1). The incident solar power on the receiver $Q_{\text{solar,in}}$ is usually defined as the contributions of each heliostat, as defined in Equation (1).

$$Q_{\text{solar,in}} = \text{DNI} \sum_{i=1}^{N} A_{h,i}\, \eta_{\text{cos},i}\, \eta_{\rho,i}\, \eta_{\text{track},i}\, \eta_{\text{atm},i}\, \eta_{\text{spill},i} = \text{DNI}\, A_{\text{field}}\, \eta_{\text{opt}} \tag{1}$$

where N is the total amount of heliostats in the field; A_h is the reflective area of the heliostat; η_{cos} is the cosine efficiency that accounts for the losses caused by the projection of the incoming radiation; η_{track} is the tracking efficiency accounting for the losses caused by errors during aiming; η_{atm} refers to the efficiency of the atmospheric transmittance; and η_{spill} refers to the spillage efficiency, which is caused by the fraction difference between the power being reflected from the mirror and that actually strikes the receiver. The collection of heliostats in the system is referred to as the heliostat field, and the contribution of the different efficiencies can be added into the optical efficiency, leading to a simplified version of the $Q_{\text{solar,in}}$, as defined in Equation (2).

$$Q_{\text{solar,in}} = \text{DNI}\, A_{\text{field}}\, \eta_{\text{opt}} \tag{2}$$

At the receiver, the concentrated solar radiation is absorbed and converted into thermal energy, increasing the enthalpy of the heat transfer fluid (HTF) circulating within the system. The receiver thermal efficiency is given by Equation (3).

$$\eta_{rec} = \frac{\dot{m}\, c_p (T_{\text{out}} - T_{\text{in}})}{Q_{\text{solar,in}}} \tag{3}$$

where $\dot{m}$ is the HTF mass flow rate, c_p is the specific heat capacity, and T_{out} and T_{in} are the HTF outlet and inlet temperatures, respectively. The high-temperature HTF is then used to drive a cyclic thermal process, such as a conventional power block, to generate electricity or provide process heat.

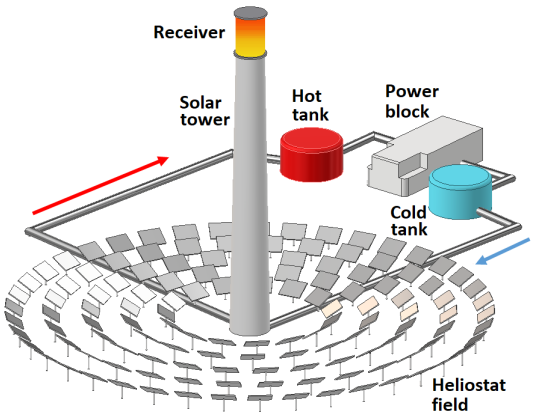


Figure 1. Typical CST tower plant configuration.

Additionally, before entering the power block, the HTF can be stored in a Thermal Energy Storage (TES) system, which captures excess thermal energy produced during periods of high solar radiation. This stored energy allows CST tower systems to continue generating electricity even when solar radiation is unavailable, thereby enhancing dispatchability, improving grid integration, and contributing to the stability and reliability of the power grid.

4. Solar Tower Receiver Systems

The receiver in a CST tower system is the key component responsible for capturing and converting concentrated sunlight into high-temperature thermal energy, which is then transferred to a heat transfer fluid (HTF) circulating through the receiver. A comprehensive review of the advancements in central receiver systems for CST was conducted by Ho [22]. While receiver designs vary based on technical and operational requirements, they are commonly classified by geometry into three main categories: external receivers, cavity receivers, and volumetric receivers [23]. Among these, external receivers are the most widely used in large-scale commercial CST applications. Approximately 50% of the total cost of a CST plant is attributed to the heliostat field, while the receiver accounts for around 20%. Despite its lower cost share, the receiver is a critical component, as it operates under extreme thermal and mechanical conditions. These factors underscore the importance of properly sizing the receiver to ensure that the heliostat field is not oversized, while maintaining the durability and efficiency of the receiver throughout its useful life. The receiver design process involves multiple considerations, with the choice of material and heat transfer fluid (HTF) playing a key role. These factors influence the operating temperature limits of the receiver, the heat transfer capacity, and the resistance to mechanical stress, among other characteristics [24,25]. Traditionally, receiver designs rely on standard heat flux distributions for thermal, mechanical, and hydrodynamic analyses, with the process largely guided by the experience of the designer. Ultimately, the optimal receiver design is typically selected based on either maximum thermal efficiency, minimum levelised cost of energy (LCOE), or as a combination of these two factors.

It should be mentioned here that other types of CST receivers, such as falling-particle and solid-media receivers, have been proposed and are currently being explored in academic research [26]. However, these concepts remain in relatively early stages of development, with limited or no commercial deployment. Moreover, while a few studies discuss the use of AI in broader CST contexts, to the best of our knowledge, there are currently no published works specifically applying AI-driven generative design optimisation to these emerging receiver types. For this reason, the present review focuses exclusively on cavity, external, and volumetric receivers, where such optimisation approaches have already been implemented and studied in more depth.

4.1. External Receiver Systems

External or exterior receiver systems are strategically constructed in vertical tube configurations, in which a large number of tubes is arranged in such a way as to form a cylindrical or polygonal shape. Key design considerations include the vertical length, diameter, wall thickness, and material of the tubing, as well as the tube spacing and HTF flow pattern characteristics. Inlet and outlet plenums usually connect several tubes creating arrays that, when merged, form the overall receiver system. The tubes are coated with high-absorptivity paints to absorb as much of the incoming energy as possible and avoid reflections. The HTF used in these types of receivers is usually a mixture of molten salts, liquid sodium, or water/steam for direct electricity generation when pumped in an upward direction (see Figure 2). External receivers operate at high temperatures (i.e., up to 560 °C

when the HTF is molten salts) and have a large absorber area, leading to high radiation and convective losses (between 20 and 40% of the incident energy) [23,27].

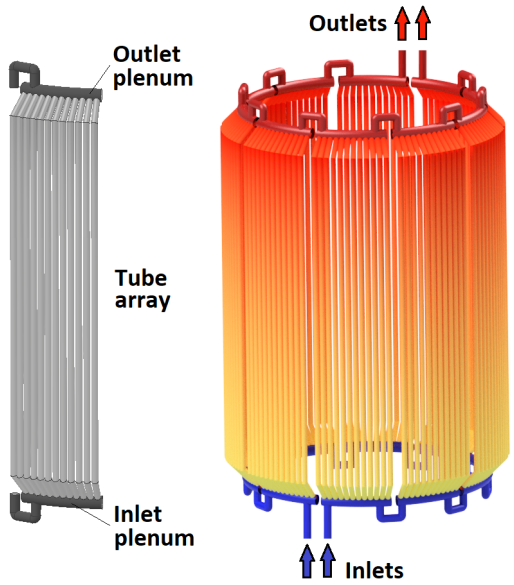


Figure 2. An example of an external receiver with its main characteristics. Cold HTF flows from the bottom inlets to top outlets.

4.2. Cavity Receiver Systems

Unlike external receiver systems, a cavity-type receiver consists of a geometrically shaped enclosed cavity with a single opening through which it receives concentrated solar radiation. Governed by several design parameters, the shape of the cavity can be of different geometries, such as conical, cylindrical, spherical, etc. Similarly to the external receiver, tubes arranged accordingly inside the cavity absorb the incoming energy and transfer the latter to the HTF running inside the tubes (see Figure 3). Usually, the walls of the cavity are surrounded by insulation to avoid convection losses. Due to the small opening, radiation and convective losses to the environment are minimised, thus resulting in higher thermal efficiencies. However, because of the inherent geometrical characteristics of cavity receivers, these impose limitations on the layout of the heliostat field and require optimised aiming strategies to avoid spillage losses.

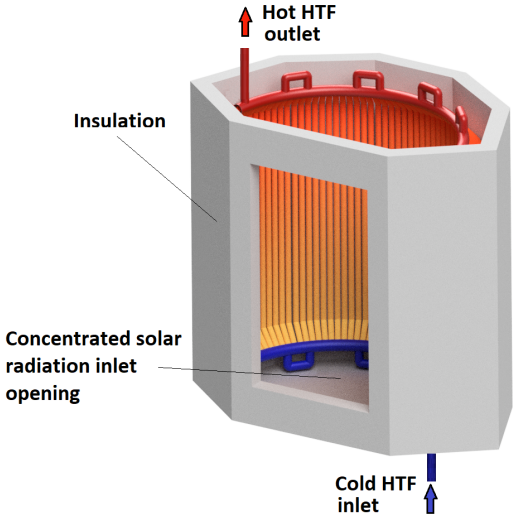


Figure 3. An example of a tube cavity receiver with its main characteristics.

Cavity receivers in which the HTF is circulated directly behind the cavity wall have also been proposed [28]. An example of such a receiver is shown in Figure 4. In this type of cavity receiver, the heat transfer fluid does not run in tubes but in a secondary cavity (designated as HTF circulation cavity in Figure 4) that is formed around the primary cavity. Heat is transferred to the fluid by convection while the fluid is circulated in the hot wall of the primary cavity. The HTF circulation cavity can be filled with porous material to enhance heat transfer characteristics, as shown in [29].

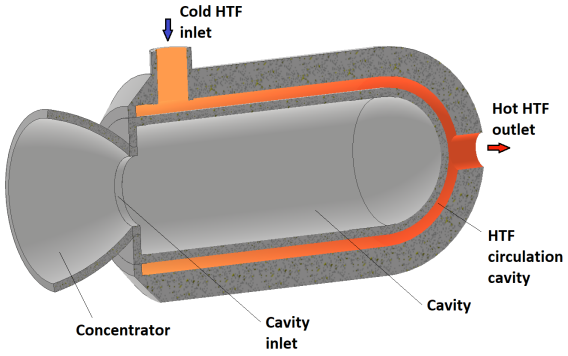


Figure 4. A cavity receiver in which the HTF is directly in contact with the walls of the cavity.

4.3. Volumetric Receiver Systems

Unlike external and cavity receivers, which absorb solar radiation primarily through their surfaces, volumetric receivers capture concentrated solar radiation in a three-dimensional manner, i.e., volumetrically [30]. To enhance energy absorption, the cavity is typically filled with porous materials such as knit-wire, foam, foil structures, or solid particles, as well as small channel arrays. These materials increase the contact area, allowing for better heat transfer along the depth of the cavity. The inlet aperture of the volumetric cavity is usually sealed using a glass/quartz window to ensure that the HTF does not escape. In volumetric receivers, as shown in Figure 5, the heat transfer fluid (HTF) is usually air or another gas that flows through the porous medium inside the cavity, where it is heated by concentrated solar radiation, leading to a rapid temperature increase. When solid particles are used, they can serve as the HTF if fluidised, or as a thermal energy storage (TES) medium due to their ability to retain heat, a property known as thermal inertia.

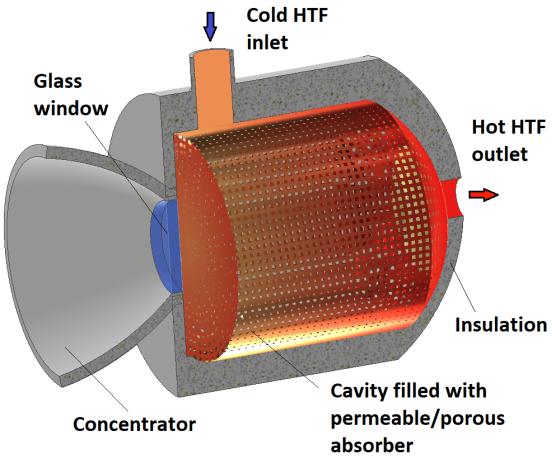


Figure 5. A typical porous volumetric receiver with its main characteristics.

5. General Overview of AI Techniques Employed in the Generative Design of CST Tower Receivers

This section classifies various AI methods and techniques commonly used in the generative design of CST tower thermal receivers, as identified through the literature review. To enhance reader understanding, each AI technique is briefly introduced, followed by a concise explanation of its operational characteristics.

5.1. Metaheuristic Algorithms

Metaheuristic algorithms are general problem-solving approaches that guide the search process to efficiently explore the search space, particularly when dealing with complex, large-scale, and non-deterministic problems. Unlike exact optimisation methods, which guarantee the identification of the optimal solution, metaheuristics focus on finding good solutions within a reasonable time frame. A key characteristic of all metaheuristic algorithms is the division of the search procedure into two distinct phases: exploration, which involves a broad investigation of the search space, and exploitation, which focuses on a more localised search in promising regions identified during the exploration phase.

In every problem solved using metaheuristic algorithms, there exists multiple decision variables and one or more objective functions. The goal of the algorithm is to find the solution (value for each decision variable) that results in the optimal value of one or more objective functions. Depending on the algorithm jargon, the proposed solutions can also be referred as individuals, particles, etc., and the decision variables as the genes or characteristics each solution owns. While each algorithm has its own characteristics and methods, all of them require the initialisation of certain variables before the optimisation begins (such as population or swarm size, coefficients, etc). These set-up parameters, which are not externally influenced during the optimisation, are also referred to as the hyperparameters.

These algorithms are typically classified into three main categories: Evolutionary Algorithms (EAs), Swarm Intelligence (SI), and physics-based methods. A brief description of each method is given below.

5.1.1. Evolutionary Algorithms

Evolutionary Algorithms (EAs) are typically inspired by the natural process of evolution, based on Darwin's theory. The main representative of evolutionary algorithms are Genetic Algorithms (GAs). These are search and optimisation algorithms inspired by the principles of genetics. These algorithms aim to replicate the biological processes of natural selection and adaptation to the environment. GAs are particularly well-suited for solving complex problems with large search spaces. Holland [31] defined the key components and principles of a genetic algorithm, including fitness evaluation, parent selection, crossover, mutation, and inversion processes.

In brief, the process begins by generating a population of individuals (commonly between 50 and 200 candidates), each represented as a chromosome (e.g., a real-valued vector). The population is then evaluated based on specific objectives during the fitness evaluation stage. The next generation is created through parent selection (often using methods like roulette wheel or tournament selection), where only individuals with better fitness pass on their genes to the next generation. Once parents are selected, their genes are combined during the crossover, which is applied with a probability typically ranging from 0.6 to 0.9. In the mutation process some genes are randomly altered to increase population diversity, applying a relatively low probability, usually between 0.001 and 0.2. Figure 6 illustrates a typical flowchart of a GA, demonstrating the repeated reproduction process until convergence.

Variations of GA-based optimisation algorithms have also been proposed and utilised. For example, Krishnakumar [32] introduced a GA variation called micro Genetic Algorithm (mGA or μGA), which allows the use of smaller populations, i.e., 5 individuals, compared to the population of 30–200 individuals usually employed in GA. In the mGA, a new process called elitism is introduced, in which the best individual is included in the next generation with no alteration of its genes, and the mutation operator is not used. Another variant is the "non-dominated sorting genetic algorithm (NSGA)" that was presented by Siinivas and Deb [33], which is able to better address multi-objective optimisation problems. NSGA incorporates the concept of non-dominated sorting to rank the best solutions in a population. A solution is considered to dominate if it outperforms, and the best solutions are then the non-dominated ones. Building upon NSGA, two more variations, NSGA-II and NSGA-III, were defined in Deb et al. [34] and Deb and Jain [35], respectively.

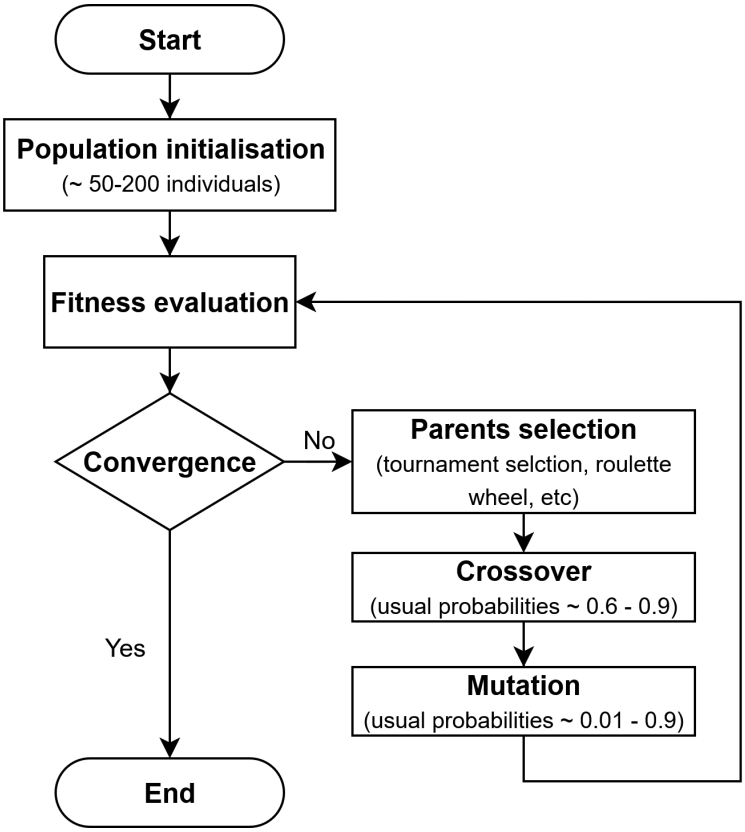


Figure 6. Typical genetic algorithm flowchart. Rounded boxes represent starting/ending points, rectangular boxes represent processes, and the diamond box represents a decision process.

5.1.2. Swarm Intelligence

Swarm Intelligence (SI) algorithms are population-based stochastic optimisation algorithms inspired by the social behaviour, modelling the collective behaviour of decentralised, self-organised systems like humans or animals. They are particularly useful for optimisation problems with a large solution space, and their simplicity and ability to escape local optima make them a popular choice for various applications, including engineering design, parameter tuning, and machine learning optimisation.

Particle Swarm Optimisation

Particle Swarm Optimisation (PSO) methodology, presented by Kennedy and Eberhart [36], is based on behaviours observed in bird flocks or fish swarms that exhibit individual and collective group dynamics and intelligence when optimally searching for food. The behaviour of each particle in the swarm is mimicked along several time steps,

being defined by three attributes: position, velocity, and the personal best position, which is the best solution in all time steps carried out so far. The position and velocity of all the particles in the swarm are randomly initialised. The fitness evaluation is carried out and the best global position is defined as the best solution of the swarm in all time steps that participate in the guidance of all the particles.

Krill Herd Optimisation

The krill herd optimisation (KHO) algorithm, first introduced by Gandomi and Alavi [37], is inspired by the random movement and social interaction observed in the herding behaviour of Antarctic krill. In this algorithm, the position of each krill represents a potential solution in the optimisation process. The movement of each krill toward a food source is determined by three main processes: movement influenced by the presence of other individuals, foraging activity, and random diffusion. Additionally, two genetic operators—crossover and mutation—are incorporated to enhance solution diversity. The flowchart of the optimisation process is illustrated in Figure 7.

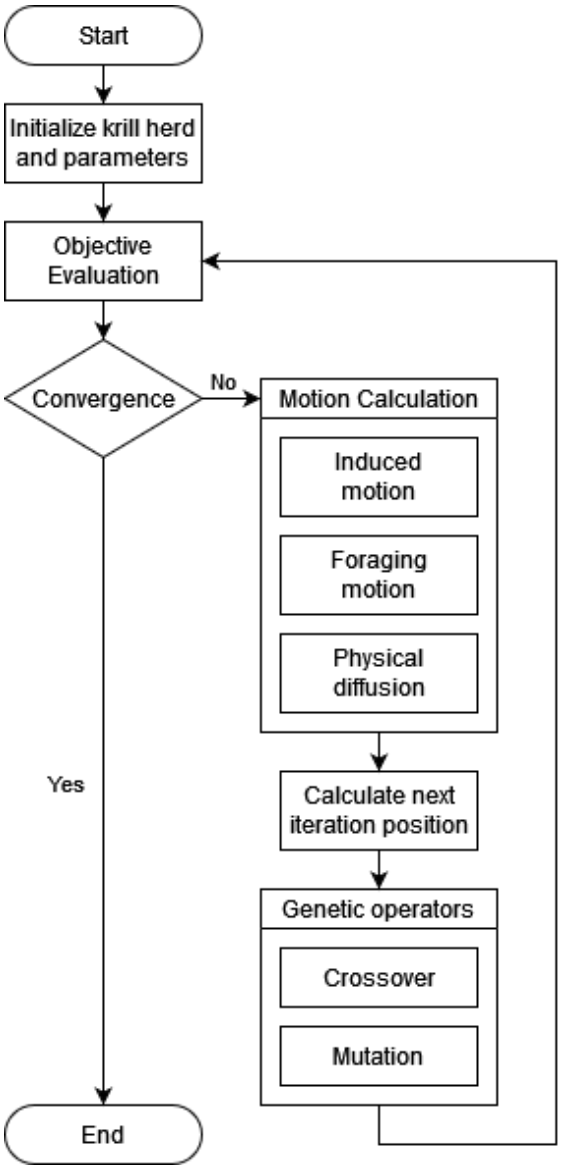


Figure 7. Krill herd optimisation algorithm flowchart (adapted from: [37]). Rounded boxes are starting/ending points, rectangular boxes are processes, and the diamond box is a decision process.

Grey Wolf Optimiser

Developed by Mirjalili et al. [38], the Grey Wolf Optimiser (GWO) algorithm is inspired by the leadership hierarchy and hunting behaviour of grey wolf packs. The pack is structured into four ranks—alpha, beta, delta, and omega—in decreasing order of dominance. The hunting process is modelled through three main steps: searching, encircling, and attacking the prey. In the algorithm, the alpha, beta, and delta wolves (representing the best solutions) guide the pack toward the prey, which corresponds to the global minimum. However, since the exact location of the prey is often unknown, it is approximated based on the positions of these leading wolves. Exploration primarily occurs during the searching and encircling phases, while exploitation is emphasised in the final iterations during the attacking phase.

Teaching–Learning-Based Optimisation

The Teaching–Learning-Based Optimisation (TLBO) algorithm was first introduced by Rao et al. [39] for optimising mechanical design problems and later enhanced by Rao et al. [40] to address large-scale non-linear optimisation challenges. TLBO is inspired by the influence of a teacher on students in a classroom setting. In this algorithm, the population is conceptualised as a class of students (learners), with the objective functions representing different courses. The optimisation process is divided into two phases, the Teacher Phase and the Learner Phase, iterating over multiple cycles. (i) Teacher phase: the best-performing student is designated as the teacher, who aims to elevate the knowledge level of the entire class. (ii) Learner phase: students improve their knowledge by interacting and exchanging information randomly among themselves.

5.1.3. Physics-Based Optimisation

Physics-based algorithms are inspired by natural physical laws, such as gravitational force, electromagnetic interactions, buoyancy, and atomic orbital models, among others. These algorithms leverage physical principles to guide the optimisation process and solve complex problems efficiently.

Simulated Annealing Optimisation

Originally defined by Kirkpatrick et al. [41], the Simulated Annealing (SA) optimisation method is inspired by the annealing process in metallurgy. During annealing, a metal is heated until it melts and then slowly cooled, spending significant time near its freezing point to prevent crystal defects. The SA algorithm begins by setting an initial temperature, which gradually decreases over iterations. In each iteration, a potential solution is randomly generated. The objective function is represented as the system's energy, which must be minimised throughout the annealing process until the system stabilises (freezes) and no further changes occur. To prevent abrupt energy changes that could lead to crystal deformations, leading to quenching, the probability of accepting a new solution is given by a probability function. This probability function allows for broader solution acceptance in the early stages when the temperature is high, enabling extensive exploration of the search space. As the temperature decreases, the algorithm shifts towards exploitation, refining the solution to avoid local minima, mimicking the controlled cooling process that prevents defects in annealed materials.

5.2. Fuzzy Logic Inference

In contrast to classical logic, where binary values 0, 1 define the status of a variable, the fuzzy logic approach deals with imprecision by deriving conclusions from variables considered to have a degree of truth (in the range [0–1]), so the setting boundaries are

blurred. Fuzzy logic inference (FLI) optimisation is based on fuzzy sets and rules to optimise complex systems with high uncertainties. During the optimisation, the relevant variables are first fuzzified to later define the fuzzy rules and enable the system to generate the fuzzy outputs. Finally, during the defuzzification step, the fuzzy outputs are converted into concrete values of the real system being modelled.

5.3. Artificial Neural Networks

Artificial Neural Networks (ANNs) are computational models inspired by the organisational principles of the human brain. They are used to identify correlations and patterns efficiently, without the need to solve complex differential equations, by learning from known data. An ANN consists of multiple layers of interconnected artificial neurons, also known as perceptrons. Each neuron functions as a data processing unit: it receives one or more input signals, applies weights to these inputs, sums them, and then processes the result through an activation function, such as sigmoid, hyperbolic tangent, softmax, ReLU, etc., to generate an output. A schematic representation of a neuron structure is shown in Figure 8.

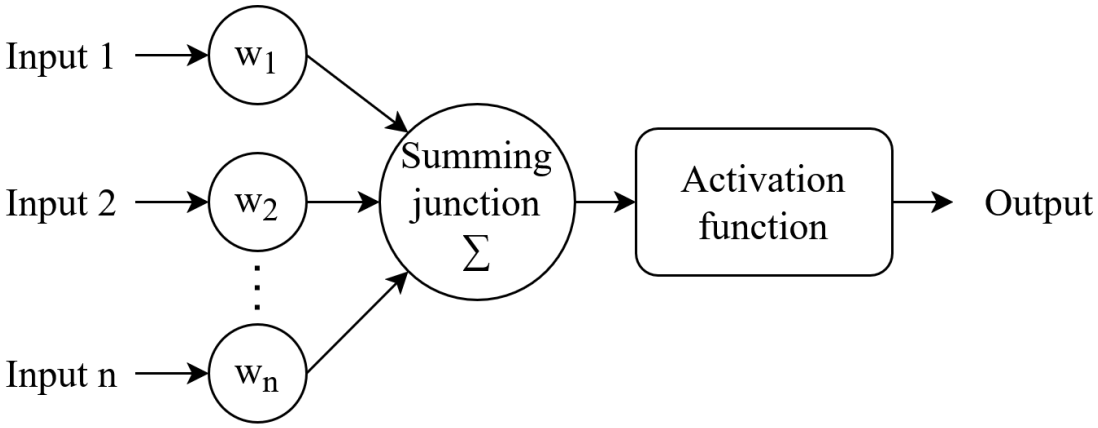


Figure 8. Schematic representation of a neuron structure.

6. Generative Design of CST Receivers

This section presents an exhaustive and comprehensive review of the application of AI-based generative design optimisation for CST receivers. The section is divided into three sub-sections, each reviewing relevant studies focusing on the three different types of receivers, i.e., the cavity, external, and volumetric receivers.

6.1. Cavity Receivers Optimisation

In the design process of cavity receivers, the primary focus is on thermal efficiency, aiming to maximise the energy absorption while minimising heat losses to ensure optimal performance. However, during this process, several key design considerations are taken into account. These include structural and material considerations, meaning that the design must account for thermal expansion, corrosion resistance, and durability to ensure long-term reliability, heat transfer fluid flow-path considerations to ensure efficient heat exchange while minimising pressure drops, and considerations regarding possible integration with thermal energy storage units to ensure stable operation and dispatchability.

For homogenising the radiative flux intercepted by an orthogonal inlet aperture cavity receiver, Wang et al. [42] tried to optimise the absorptivity distribution of the surfaces that constitute the receiver. The authors considered dividing the receiver surface into active surfaces, as shown in Figure 9a, while the active surfaces themself were further subdivided into 36 different interdepended sections. The NSGA-II algorithm was then employed to find receiver geometry solutions that minimise the radiative flux variation and reflection

losses. The performance of each candidate receiver geometry was evaluated at 15 different sun positions, i.e., five specific hours of the day at spring equinox and summer and winter solstice. The results generated by the algorithm showed that the optimal absorptivity distribution across the receiver surface is somehow opposite to the distribution of the projected solar radiative flux onto the receiver surfaces, as observed in Figure 9, i.e., wherever there is low solar irradiation the reflectivity should be high and vice versa.

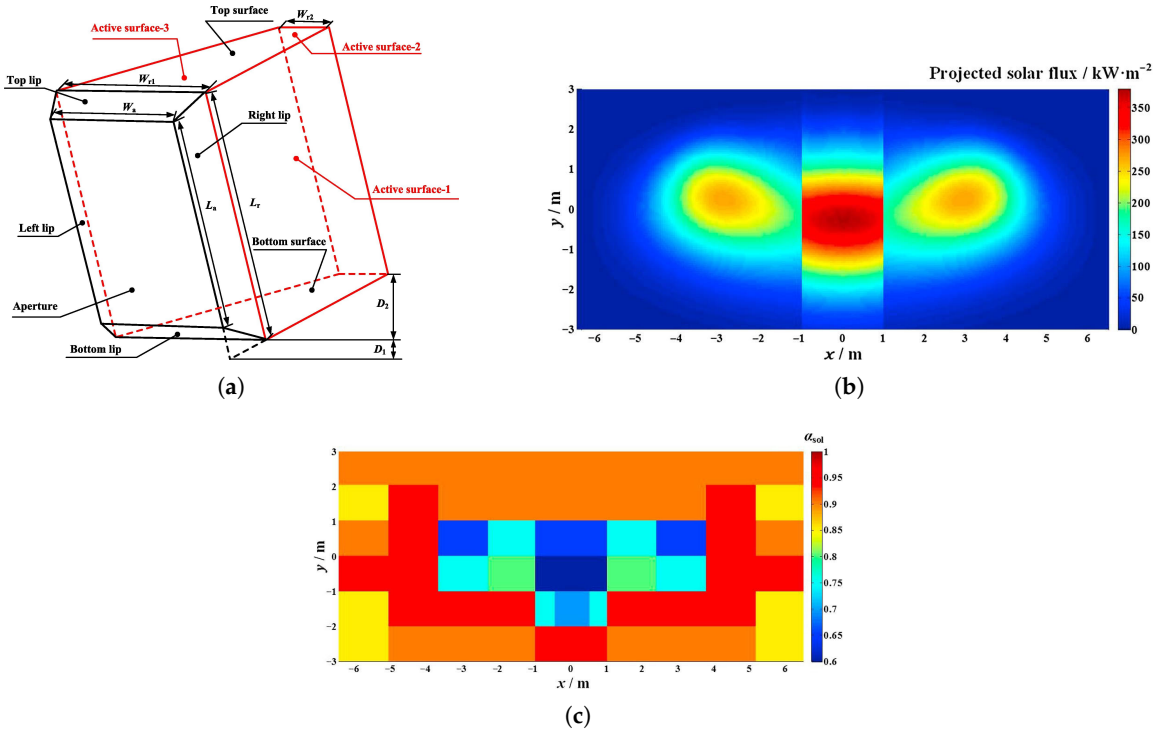


Figure 9. Cavity receiver optimisation, as performed by [42]: (**a**) overview of the receiver geometry, (**b**) the resulting optimal absorptivity distribution on the unfolded active surfaces of the receiver, (**c**) the corresponding distribution of the average solar flux on the unfolded active surfaces of the receiver. (Reprinted from [42] with permission from Elsevier).

To tackle illumination and radiative heat transfer problems, Asselineau et al. [43] presented a stochastic optimisation algorithm in conjunction with Monte Carlo ray tracing. The process allowed identifying the best performing geometrical configurations within a population, while a heuristic component of the algorithm was able to discard underperforming candidates immediately when identified. The authors applied the methodology for the design of an axisymmetric cavity receiver for direct steam generation. The axisymmetric receiver geometry was parametrised using a set of axial coordinates set along the axis of rotation of the receiver, as shown in Figure 10a. The results indicated that the methodology was able to generate optimal receiver geometries with significantly reduced computational cost (usually arising from intensive ray-tracing simulations) due to the heuristic component of the methodology, which discards badly performing receiver designs early in the optimisation process, as shown in Figure 10b. In a further study, the same team also employed the stochastic optimisation methodology with the integration of hydrodynamic considerations by including a single coil tube around the internal walls of the cavity in which the water/steam was circulating [44]. For this approach, the cavity was parametrised with only four parameters, as shown in Figure 10c. The coil tube was discretised as a helical path conforming to each candidate receiver geometry, while a dedicated heat transfer model was developed to account for the energy balance over the tube elements. It was concluded that the optimisation process was able to converge to receiver geometries that optimise

the radiative losses, while being able to minimise the computation effort of the Monte Carlo ray-tracing step, i.e., intensive ray tracing was only performed on promising receiver candidates, enabling and then performing refined energy balances only to those promising receiver candidates.

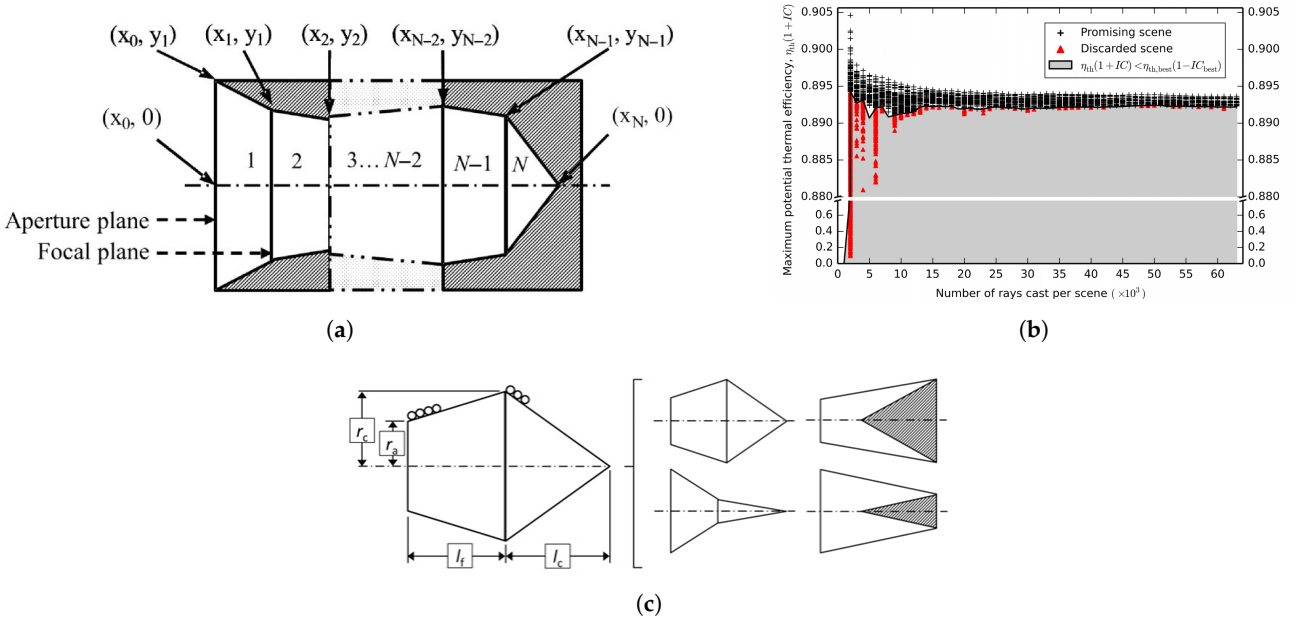


Figure 10. Axisymmetric cavity receiver geometrical optimisation, as performed by [43,44]: (**a**) receiver parametrisation via axial points along the axis of rotation, (**b**) plot showing the convergence of the stochastic optimisation process. Notice that the number of rays cast for the Monte Carlo ray-tracing step continuously increases for testing promising receiver candidates, while badly performing candidates are discarded early during the optimisation process, (**c**) receiver parametrisation using four parameters. (Figures (**a**,**b**) reprinted from [43] with permission from Optica Publishing Group, figure (**c**) reprinted from [44] with permission from Elsevier).

Loni et al. [45] employed a combination of numerical modelling and an ANN for optimising the structure of a tubular cavity receiver. Considering the tube diameter, cavity depth, and solar irradiance, the objective of the study was to predict the thermal performance of the receiver using a thermal model developed specifically for the receiver. The authors first employed experimentally validated numerical results to train the ANN, and then used the ANN to derive the optimum structure of the receiver in terms of maximising its thermal performance. The study reports an almost perfect agreement between the ANN predictions and numerical results at a low computational cost.

Similarly, an ANN was also employed by [46] for predicting the radiative and convective losses of a semi-spherical cavity receiver investigating the effects of several parameters including the diameter ratio between the inlet aperture diameter and the diameter of the spherical section, the receiver's angle of inclination, its operating temperature, the insulation thickness, the emissivity, and the air density. Upon investigating the heat losses for different receiver geometries using numerical modelling, the authors used the ANN to see whether was capable of predicting the heat losses for a large set of influencing parameters as discussed above, yielding a large combinatorics set. The authors reported that the ANN modelling was able to significantly improve the Nusselt number correlations for the convective, radiative, and total heat losses.

A combination of an EA and an ANN was used by Schöttl et al. [47] in an attempt to simultaneously optimise optical, thermohydraulic, and operational aspects of a tubular cavity receiver geometry with a rectangular inlet aperture. The optimisation procedure involved several cavity geometrical parameters, including its width, height, lip height, tilt

angle; hydraulic parameters, including the number of panels and tubes per panel; and optical parameters, including the aiming strategy on the inlet aperture plane. Figure 11a depicts a snapshot of the initial receiver geometry and its parametrisation variables. A custom EA adapted for the needs of the study was used for accelerating the annual energy yield assessment, which was later used as a figure of merit during the ANN optimisation process. The workflow developed was then applied for the optimisation of a small-scale molten salt cavity receiver for a given heliostat field of 55MWth power, similar to the PS10 heliostat setup. The results shown reported an increase in the annual energy yields close to 4% for the optimised receiver solution, as compared to the reference receiver design used in the PS10 setup. Figure 11b illustrates the heat flux distribution for the generated optimal receiver design.

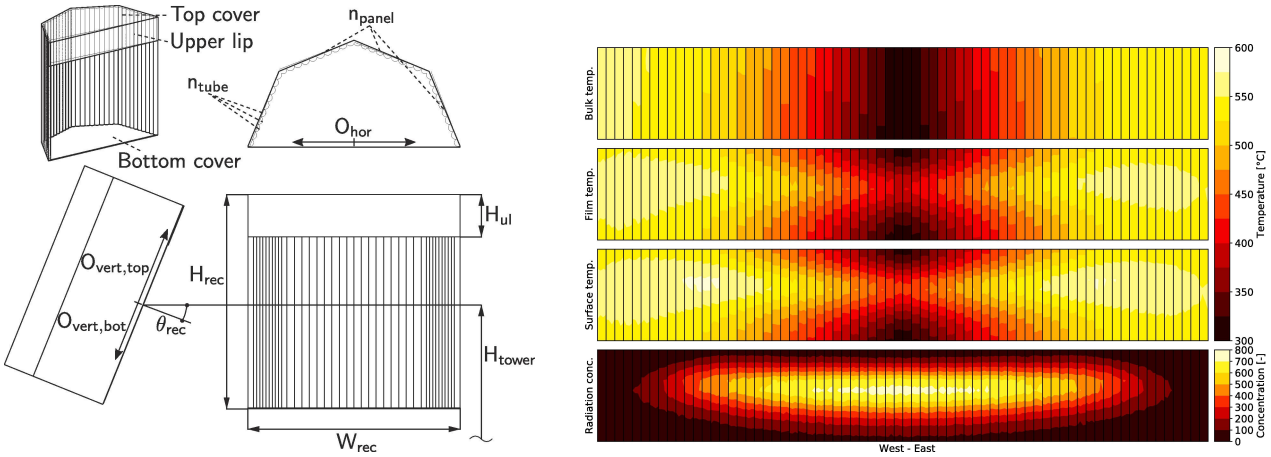


Figure 11. Molten salt tubular cavity receiver design optimisation, as performed by [47]: (**a**) overview of receiver parametrisation, (**b**) optimal heat flux distribution within the cavity obtained for the generated optimal receiver geometry.

In a study performed by [48], the authors employ four different metaheuristic optimisation methods, i.e., a GA, a PSO, an SA, and a GWO, to optimise the design and operation of a cavity receiver using air as the HTF conceived for operation with a Brayton power cycle. The receiver, shown in Figure 12a, consists of an axisymmetric cavity, in which a number of tubes is arranged around the periphery of the internal cavity wall. An MLP-ANN was used to accelerate the thermal analysis of the receiver, avoiding computationally costly simulations. Key receiver parameters included during optimisation were the inlet aperture diameter, the bottom diameter, the length of the cavity, the tubing diameter number, the total incident energy, and the HTF's inlet temperature and flow rate. On the other hand, the outputs of the ANN included the HTF outlet temperature, the thermal efficiency, the maximum temperature of wall tubing, and the associated pressure drop. After employing artificial and experimental data to train the ANN, the authors carried out multiple optimisations using the metaheuristic algorithms for optimising the aiming strategy along with the structure of the receiver (Figure 12b). The authors conclude that their approach provides an excellent solution for the fast design optimisation of cavity receivers, with the potential of using this workflow for the optimisation of similar structures.

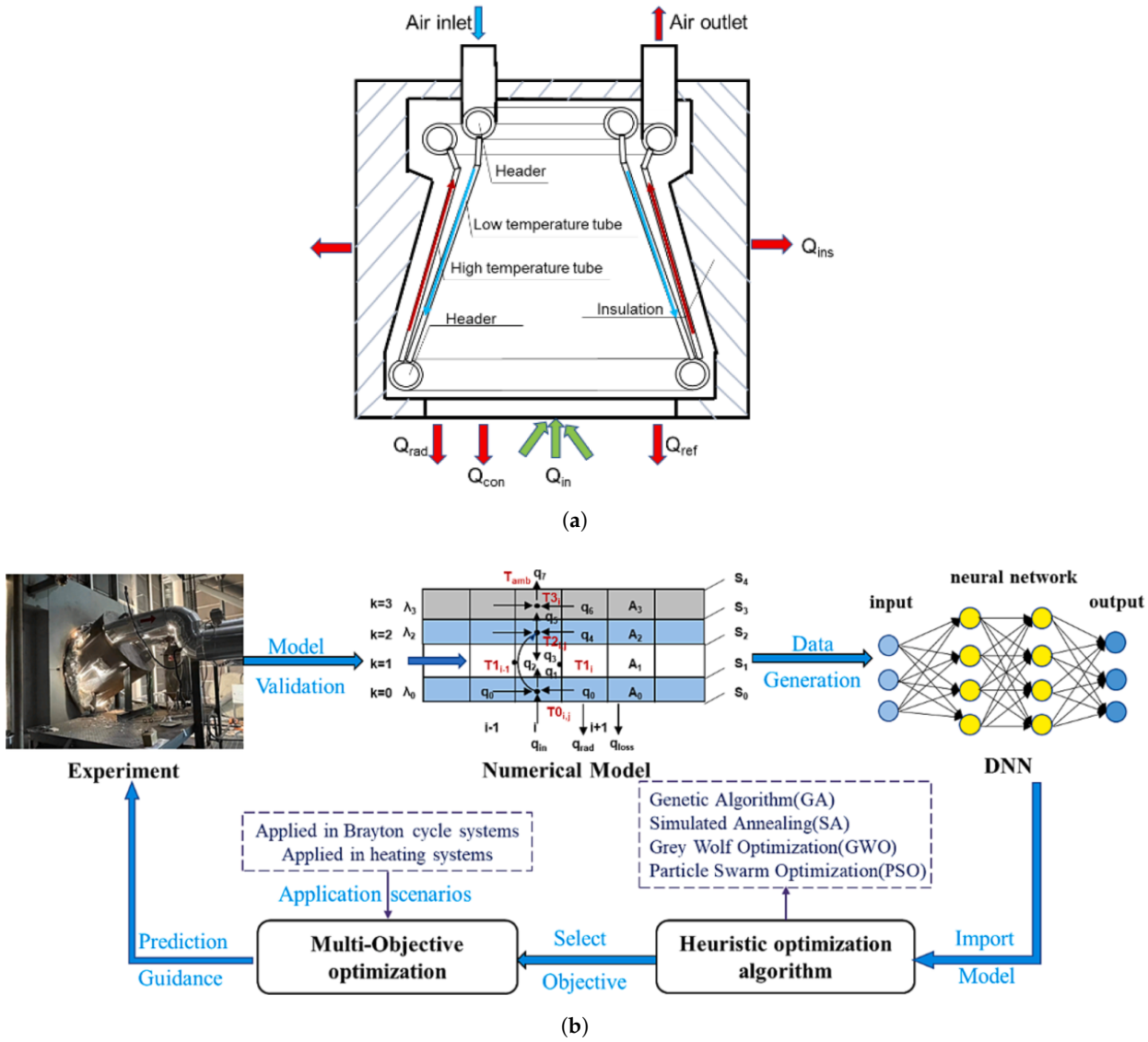


Figure 12. Cavity receiver geometry optimisation for Brayton air cycle application, as presented by [48]: (**a**) overview of the receiver geometry, (**b**) the workflow employed for the optimisation of the receiver. (Reprinted from [48] with permission from Elsevier).

Radiative enclosures can be classified as a type of cavity receiver in the context of solar energy and thermal applications, as they share similar design principles. These enclosures are specifically engineered to confine thermal radiation within an enclosed or semi-enclosed space, thereby enhancing absorption efficiency and minimising heat loss. Given their functional and conceptual alignment with cavity receivers, this review also includes studies focused on their optimisation to ensure a comprehensive analysis.

For optimising the uniformity of thermal conditions over the shape of a design body enclosed within a radiant enclosure cavity, Darvishvand et al. [49] employed Monte Carlo ray tracing in conjunction with a GA. In this problem, an asymmetrical and irregular-shaped design body is positioned within a cavity whose top wall is equipped with a set of radiant heaters. The task was to solve the radiative heat transfer problem of finding the optimal combination of the heater's temperature and location of the design body within the cavity. While Monte Carlo ray tracing was used for the calculation of the heat flux over the design body, the GA was used for finding the optimal combination of the heater's temperature and design body location to achieve uniform flux distribution on the design body. It was shown that the methodology employed was successfully able to converge

to heat flux distributions over the design body that align very well with the desired ones, concluding that such methodologies are highly efficient for three dimensional radiant cavity enclosure design optimisation.

Another radiant cavity enclosure optimisation problem was studied by [50], in which the problem of optimising the shape of the enclosure for achieving a desired heat flux distribution was addressed. The formulation of the problem involved three surfaces, the heater surface, the design surface, and the radiant enclosure cavity surface, as illustrated in Figure 13a. All three surfaces are further segmented to facilitate increased resolution for more thorough analysis. Given a fixed heater position and a fixed design surface, the objective was to find the optimal radiant enclosure shape that achieves a uniform heat flux distribution across the design surface, close to a predefined value. The surface of the radiant enclosure was defined by control points interpolated via a B-spline. The radiative heat flux on the control surface was calculated using the discrete transfer method. For optimising the surface of the radiant enclosure, a micro Genetic Algorithm (mGA) was employed, in which the control variables involved were the control points defined by distance and an angle with respect to a reference point. The objective function was defined as the sum of square residuals between the desired and estimated values of heat fluxes over the design surface segments. In terms of the specific details of the mGA, the author employed a population of six individuals and achieved optimisation with an approximate error of 1.15% after 100 generations. The same exact optimisation problem was also performed by [51], employing a PSO optimisation algorithm instead of the mGA. Their results reported an error of a lower order of magnitude when compared to the results of the mGA, but at the expense of using a swarm with a higher number of particles (between 20 and 40).

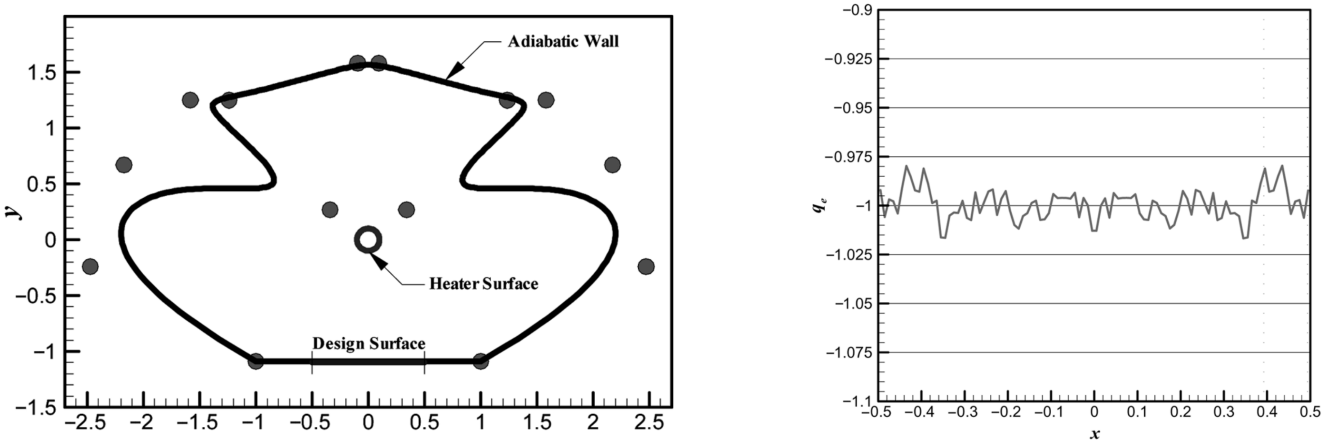
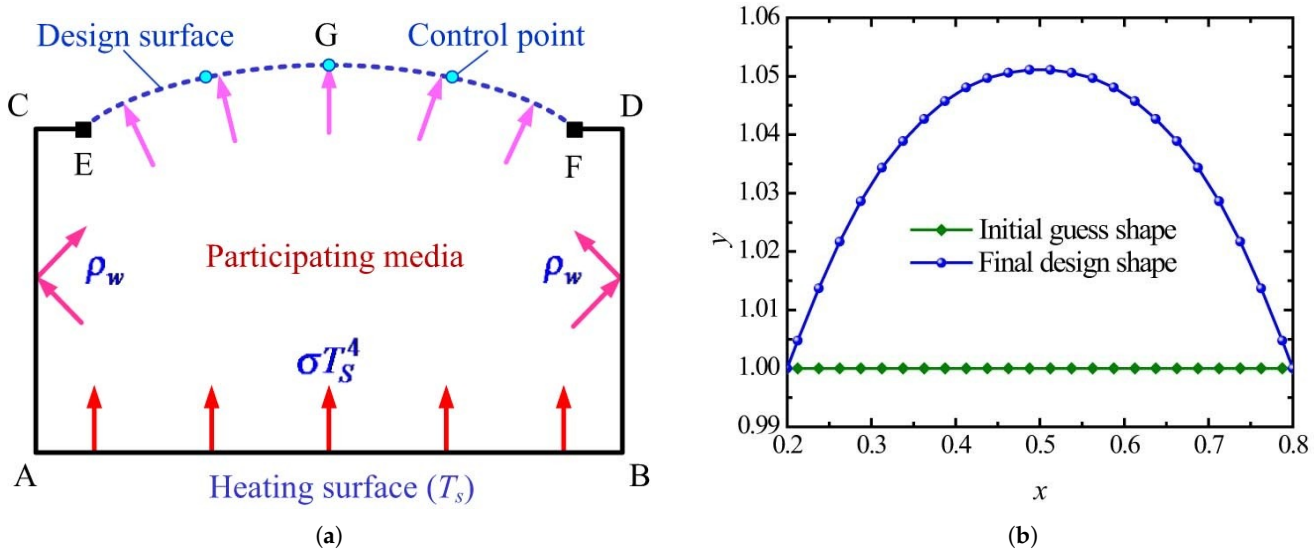


Figure 13. Optimisation of the 2D radiant enclosure, as performed by [50]: (**a**) parametrisation of the heater surface, the design surface, and the radiant enclosure surface, (**b**) optimal heat flux distribution over the design surface.

Similar to the previous study, Sun et al. [52] employed krill herd (KH) optimisation algorithms in an attempt to find the optimal design surface that achieves a uniform radiative heat flux distribution over the surface, as shown in Figure 14. For this study, the cavity was considered filled with a participating media, while the surface opposite to the design surface wall was considered as the radiating heating surface. For finding the optimal shape of the design surface, several variations of KH algorithms were investigated and compared. Although the design surface was parametrised via control points similar to studies [50,51], here, the points were interpolated using Akima cubic interpolation to approximate the surface. The results proved that KH optimisation is more efficient than the mGA and PSO

algorithms, with the relative error being approximately of the same order of magnitude as in Farahmand et al. [51]. It was shown that the best-performing version of the KH variation algorithm converged the optimisation in approximately 30 iterations with a population of 50 individuals.



(**a**) (**b**)

Figure 14. Optimisation of a 2D radiant enclosure cavity with participating media, as performed by [52]: (**a**) definition of the system configuration. (**b**) Initial and final optimised shape of the design surface achieving uniform heat flux distribution. (Reprinted from [52] with permission from Elsevier).

Moreover, Ref. [53] also applied a fuzzy logic inference (FLI) method for optimising the design surface of a cavity identical to the one used previously in [52]. The cavity was now filled with a grey participating medium. For solving the heat transfer problem within the enclosure, the discrete ordinate method was used. The optimal design surface geometry derived during the optimisation with the FLI method was compared to the ones obtained previously using the PSO and KH algorithms. While the heat flux deviation error was found to be similar in all cases, the FLI required around 20 times less computational time than the PSO and KH algorithms. The study concluded that the FLI methods are highly suitable for optimising the design of radiative enclosures that are filled with different kinds of participating media.

Simple and complex radiant enclosure cavity geometries were defined by [54] and used as case studies for performing several optimisation studies. The two enclosures are composed of a heating surface, two adiabatic walls, and a design surface. The heating surface is discretised in 30 equal-power elements. These two cavity enclosures were employed in several studies over the years, with the optimisation seeking to converge to the combination of correct heating elements to be powered in order to obtain a desired heat flux distribution over the design surface. Figure 15 shows the two cavity enclosures presented in Amiri et al. [55]. These were employed in Amiri et al. [54], Safavinejad et al. [56], Amiri and Coelho [57] using different participating media within the cavities, while using a mGA for the optimisation process. All studies concluded that the mGA performs very well, obtaining a relative error in the heat flux distribution of around 3×10^{-2} for a population of five individuals and using 300 iterations. However, the random seed selected in the optimisation has high relevance to algorithm convergence, as presented in Amiri and Coelho [57].

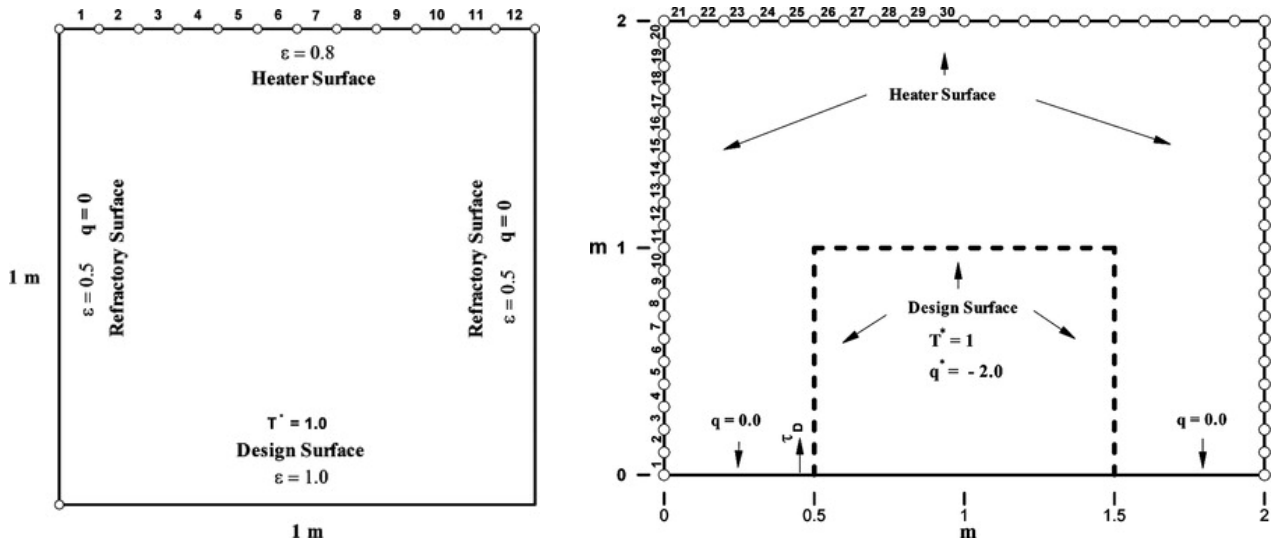


Figure 15. Definition of two radiant enclosures used as case studies, as defined by [54]: (**a**) the simple radiant enclosure, (**b**) more complex radiant enclosure.

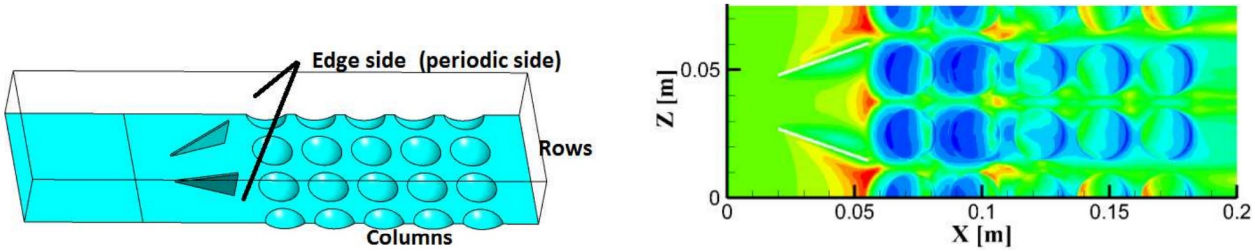
In the study by Amiri et al. [55], the problem is expanded for the optimisation of the location and heating power of the heating elements. On top of the standard TLBO algorithm, two alternative versions were also used. The results showed a better convergence with a heat flux distribution error of 2×10^{-4} when using a population of 40 individuals, also called students in the TLBO algorithm, in around 200 iterations for the simple radiant enclosure and 400 iterations for the more complex one.

Inversely to the previous studies, Payan et al. [58] solved the problem of estimating the heat flux distribution over the heating surfaces of an enclosed cavity given a desired temperature and heat flux distribution over a design surface. The cavity was also considered to be filled with grey-diffuse walls and non-grey media. The authors employed a modified discrete ordinates method to solve the radiative heat transfer problem, while two additional models were also developed for simulating the participating non-grey media. The objective function was minimised using two different methods, the conjugate gradient method (CGM) and a PSO algorithm. The reported results indicated that the PSO outperforms the CGM. This is attributed to the inherent characteristics of the CGM, which can efficiently handle continuous and linear problems; thus, the PSO performs better in the optimisation of non-linear problems, such as the one investigated in the study by Payan et al. [58].

Similarly to the previous study, Yadav et al. [59] employed an ANN to solve the inverse problem of finding the optimal spatial position and number of heaters within a two dimensional cavity/furnace filled with a mixture of CO_2 and H_2O as the participating media. As input variables to the ANN, the power of the heaters and the design surface's temperature and emissivity was used. In addition to the latter, the concentration of the CO_2 and H_2O were also used as input variables. For accelerating the optimisation process, in this study, the radiative heat transfer equation was replaced by a neural network-based surrogate model. It was shown that ANN was able to find optimal heater configurations, concluding that such methodologies are proven to be accurate, fast, and robust in solving such inverse cavity optimisation configurations.

Considering a cavity receiver in which the HTF is directly in contact with the walls of the cavity, as shown in Figure 4, Luo et al. [60] considered including dimples and delta-winglet vortex generators (DWVGs) attached on the wall of the cavity for enhancing the heat transfer performance and mixing; however, this included a penalty on the friction

factor that might lead to higher pressure losses. For evaluating the relevant HTF flow structure, heat transfer, and friction, the authors employed three-dimensional and steady-state computational fluid dynamics (CFD) simulations, while the NSGA-II algorithm was used for finding the optimal vortex generator and dimple arrangement for optimal thermal performance and efficient mixing. Several optimisation variables were considered during optimisation, including the depths and layout of the dimples and the length, height, and orientation of the DWVGs. The optimisation study converged to an optimal configuration of DWVGs and dimples that contributed to a 72% enhancement in the thermal performance of the solar receiver and that can be observed in Figure 16 .



(**a**) (**b**)

Figure 16. Integration of vortex generators and dimples over the surface of the receiver wall for enhancing thermal performance, as investigated by Luo et al. [60]: (**a**) example of the vortex generators and pimples over a circular section of the axisymmetric cavity receiver geometry. The periodic sides are used as boundary conditions in the CFD simulations to indicate that the circular section is repeated before and after the section, (**b**) example of the temperature distribution over the receiver section where cooler colours represent lower temperatures and warmer colours represent higher temperatures. (Reprinted from Luo et al. [60] with permission from Elsevier).

6.2. External Receivers Optimisation

Unlike cavity receivers, external receivers are directly exposed to the environment, making radiation, convection, and conduction losses more significant concerns. Similarly to the cavity receivers, key considerations during the design of such receivers include the velocity of the HTF within the vertical tubing, the thermal stresses that occur due to the solar radiation, the pressure drop within the tubing, erosion and corrosion considerations, etc. However, due to the inherent shape characteristics of external receivers, only a handful of studies exist that employ generative design for optimisation.

In a study performed by [61] to obtain an overall optimal configuration, a co-optimisation method that simultaneously optimises the heliostat field, the receiver, and the aiming strategy based on annual operational conditions was presented, as shown in Figure 17a. The workflow developed included an integrated optical, thermal, and mechanical model that was later used in conjunction with a GA for performing the multi-objective optimisation, aiming for the maximisation of annual solar-to-thermal efficiency conversion and minimisation of the Levelised Cost of Electricity (LCOE). For the receiver component, the receiver's diameter, height, and pipe outer diameter were variables that were considered during the optimisation process. The methodology was employed for the optimisation of a surround field tower system for which the HTF was considered to be liquid sodium. The authors reported that the simultaneous optimisation workflow resulted in an increase of 1.1% in the annual solar-to-thermal efficiency and a lower LCOE value of of 3.8% with respect to the base design. Figure 17b illustrates the net heat flux and corresponding temperature distributions over the optimal receiver design generated by the workflow.

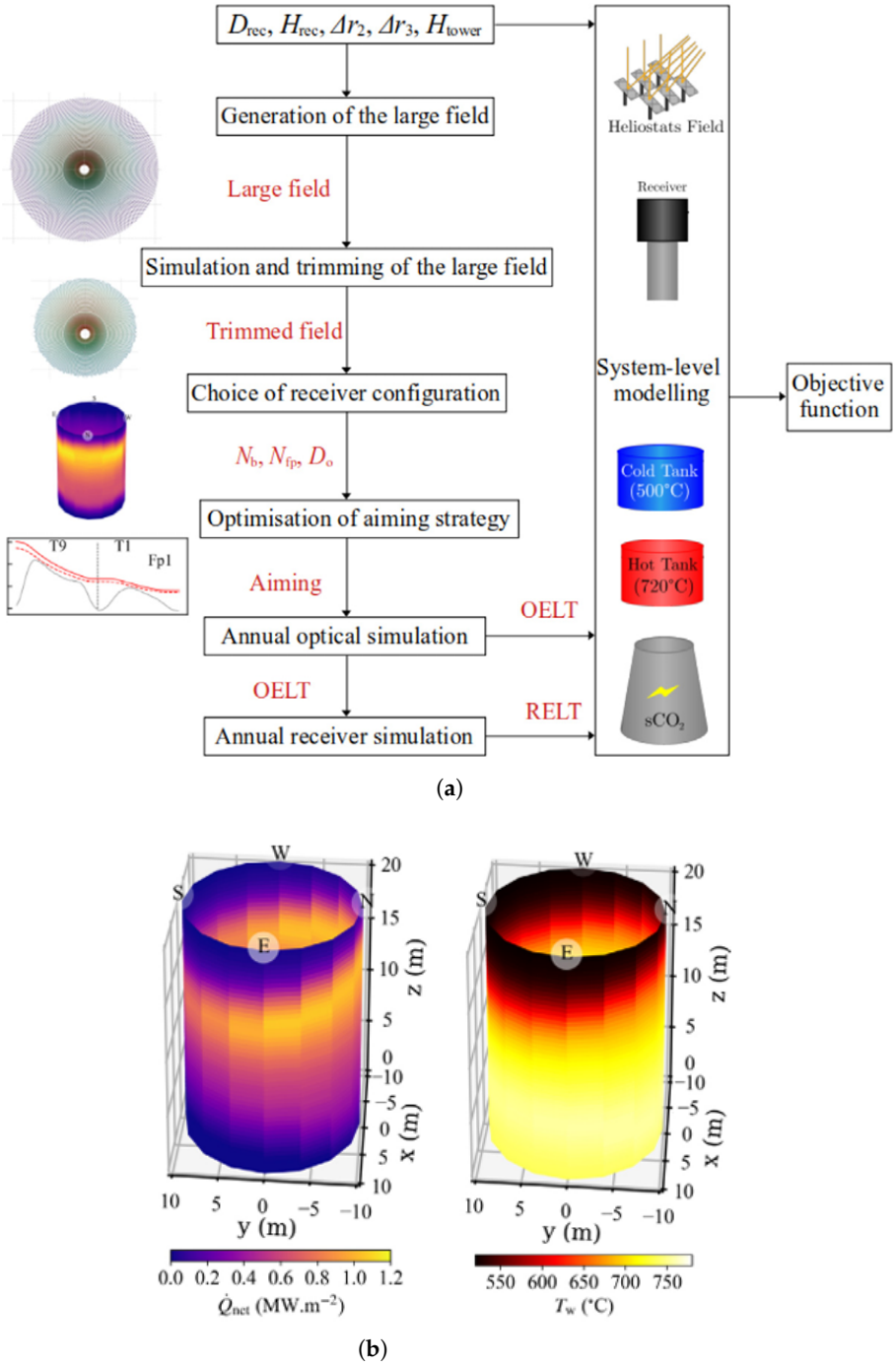


Figure 17. Simultaneous co-optimisation of the heliostat field, the receiver, and the aiming strategy of a surround field tower system, as presented by [61]: (**a**) flowchart of the annual co-optimisation methodology, (**b**) heat flux and temperature distribution over the surface of the optimally generated receiver. (Reprinted from [61] with permission from Elsevier).

As mentioned previously, thermal stresses constitute one of the key considerations when designing external receivers, since if not properly designed, these stresses can lead to early receiver failure. In an attempt to further increase the lifetime of the receiver, Moreno et al. [62] considered the use of linear actuators for inducing displacements in the longitudinal supports of the receiver, with the aim of reducing the occurring stresses, as depicted in Figure 18. The authors employed existing analytical models that were adapted retrospectively and merged, in order to be able to be integrated into a GA for optimising the lifetime of the receiver. The GA is employed twice in the same system to optimise the

displacement of the different actuators that produce minimum peak stress and optimise the rapture time due to creep. The results showed that the second optimisation problem, i.e., maximisation of the creep rupture time, gave a better performance in the increase of receiver lifetime when compared to the actuator displacement optimisation problem.

Having the maximisation of the second law efficiency, the minimisation of the receiver's area, and the minimisation of the average temperature over the receiver as objective functions, Asselineau et al. [63] employed a multi-objective stochastic optimisation algorithm to optimise the geometry of an external receiver.

The optimisation process begins with an active population of receiver designs that is evaluated multiple times, while continuously increasing the number of rays in the ray-tracing analysis of the optimisation. In every iteration, the non-dominated solutions were discarded from the active population and replaced by new proposed designs. This allowed the authors to employ a low number of rays to initially evaluate bad receiver designs, while the candidates that performed well that were not discarded were further investigated using a high number of rays in the optical analysis. This led to a significant reduction in the associated computational cost and time. Although not mentioned by the authors, the stochastic optimisation method used resembles a version of an NSGA-II that includes an increasing number of rays over the generations. The results of the optimal design for minimising the receiver area are shown in Figure 19.

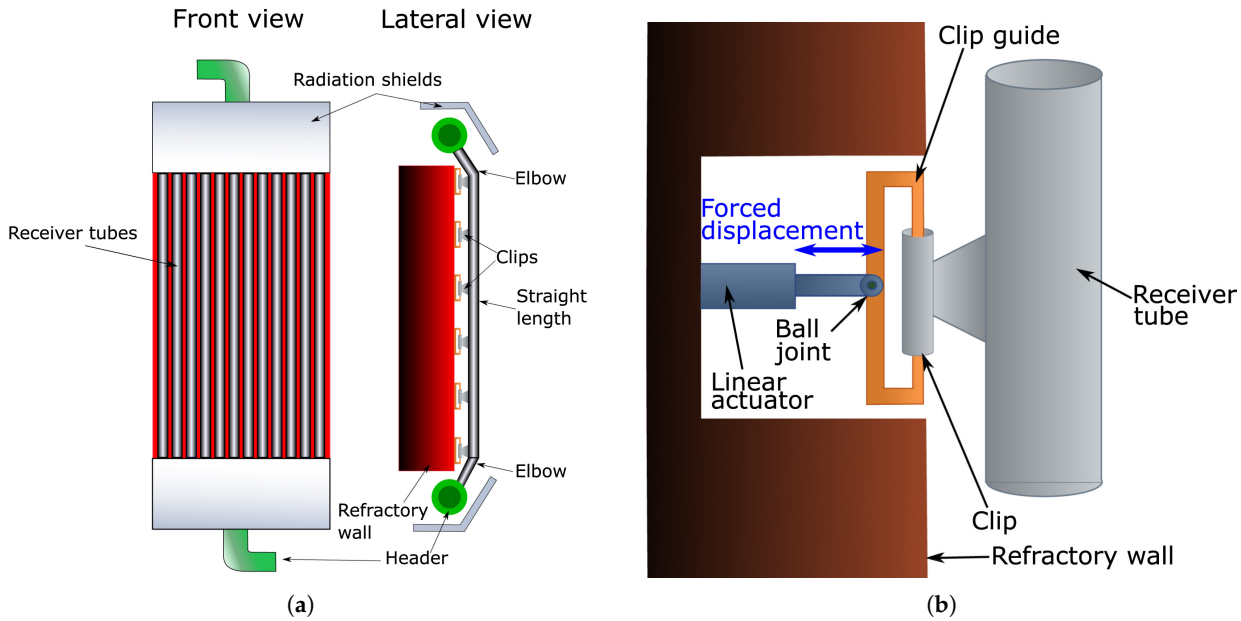


Figure 18. External receiver lifetime increment optimisation, as performed by [62]: (**a**) external receiver panel overview indicating the main components considered, (**b**) close-up view of the considered linear actuator integration for inducing displacements in the longitudinal supports of the receiver. (Reprinted from [62] with permission from Elsevier).

Finally, Hussaini et al. [64] employed GA for optimising a single-tower and a multi-tower heliostat field configuration. The optimisation process considered the coupled optimisation of the heliostat layout in conjunction with the receiver's area and tower height. The minimisation of the Levelised Cost of Heat (LCOH) was set as the objective function. The results indicated a better performance for conventional single-tower configurations in power plants with low–medium power levels (up to 350 MWth), while there was slightly better performance for the multi-tower fields in high-power power plants.

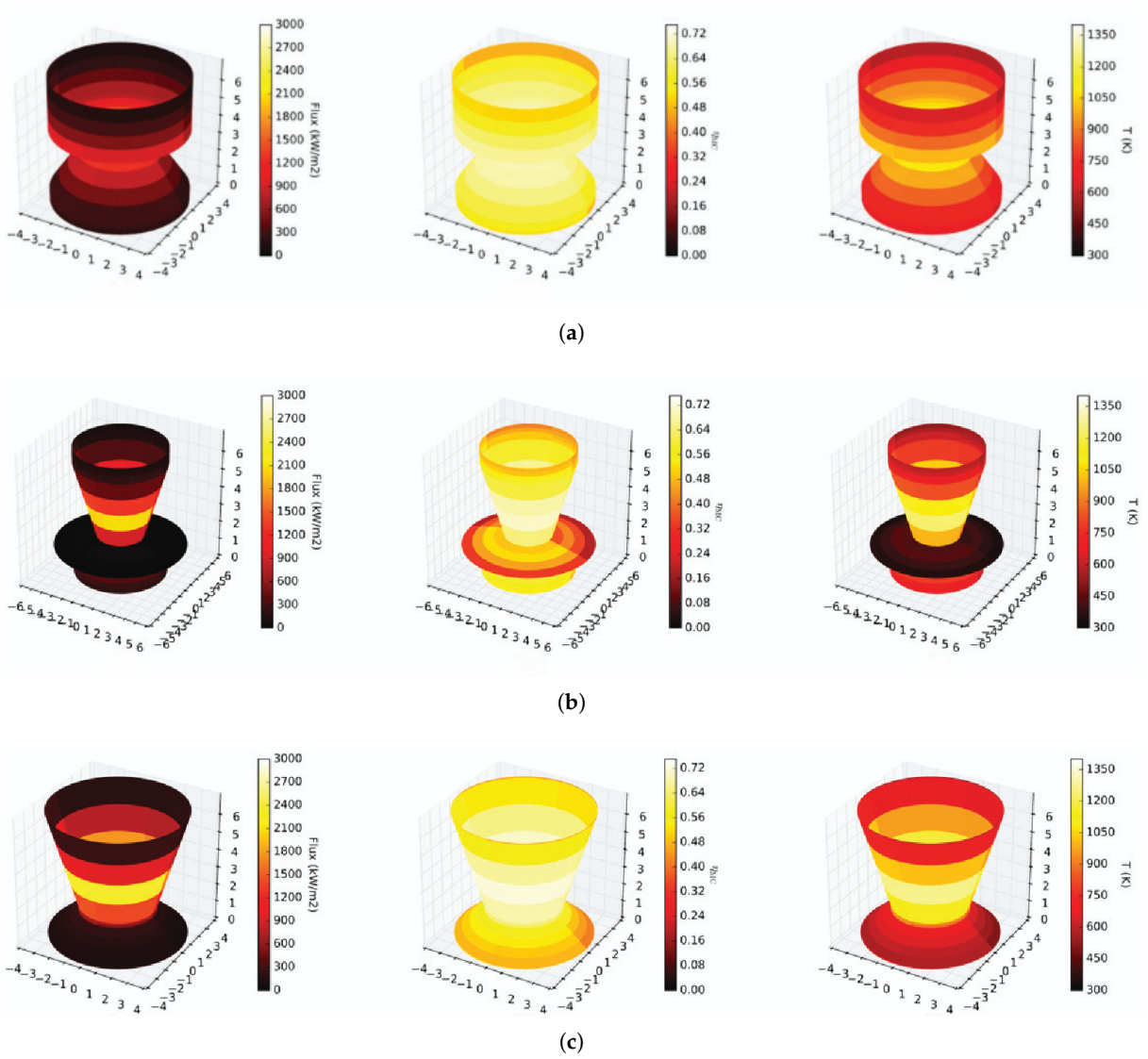


Figure 19. Optimal external receiver geometry, as performed by Asselineau et al. [63], showing from left to right, the flux distribution, the corresponding Müser–Castañs efficiency, and the resulting temperature distribution on the receiver surface. Optimal receiver geometries for the objectives of (**a**) the maximisation of work efficiency, (**b**) the minimisation of average temperature, and (**c**) the minimisation of surface area.

6.3. Volumetric Receivers Optimisation

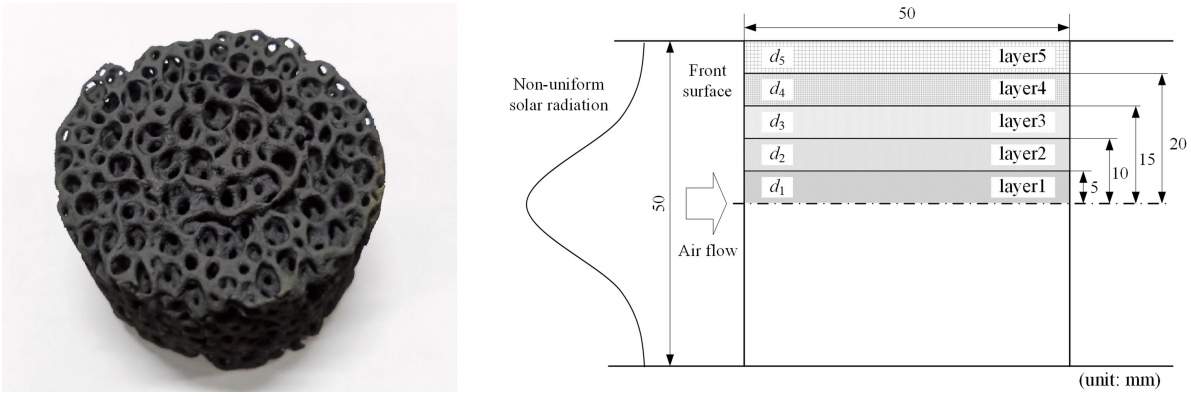
The main focus during the design of volumetric receivers is to enhance heat transfer efficiency by absorbing solar radiation in a three-dimensional manner, rather than just at the surface. Such receiver design allows for higher operating temperatures and better thermal performance, making volumetric receivers particularly suitable for high temperature solar applications, i.e., solar furnaces.

Du et al. [65] investigated the optimisation of a gradually varied volumetric receiver design. The presented configuration comprises a volumetric receiver that is composed of different porous layers. The porosity of each layer is considered to be gradually decreased from the front inlet surface to the rear surface of the cavity. The porous structure of the layers was constructed by a modified random spherical bubbles method. While employing Monte Carlo ray tracing to compute the solar radiative flux, the authors employed a GA to optimise the porosity distribution across the layers of the receiver. The objective function of the GA seeks the minimisation of the sum of the solar flux differences between adjacent

layers. The optimisation process revealed that the optimal cavity design is the one that increases the penetration of solar radiation into the porous structure, thereby enhancing volumetric absorption while minimising the heat flux gradient, an outcome likely desirable for reducing thermal stresses on the receiver.

The study was expanded by Du et al. [66] by coupling the GA with a heat transfer analysis of the porous structure to find the optimal receiver for simultaneously achieving higher thermal efficiency and minimised HTF flow resistance. After tackling the mono-objective problem of optimising the receiver porosity, pore size, and HTF inlet velocity optimal values that assure the highest thermal efficiency of the receiver, the GA was also used to tackle the multi-objective optimisation problem of finding the optimal porosity layout that assures not only a high thermal efficiency but also a low pressure drop. The authors reported that the methodology employed was able to derive receivers that optimise the flow resistance and maximise the thermal efficiency.

Furthermore, in an attempt to address the issue of non-uniform solar flux distribution on the inlet aperture of the receiver, the same team, in Du et al. [14], performed a study for the optimisation of radially graded porous receivers. In this study, the authors manufactured two-layered, radially graded porous volumetric receiver samples via 3D printing of Inconel 718 material, as shown in Figure 20a. After generating the samples, the authors performed experimental and numerical studies for evaluating the relevant heat transfer processes and fluid flow characteristics. Based on the latter results, a GA was employed for performing the optimisation of multi-layer receiver structures, i.e., five-layered graded porous receivers (Figure 20b). The results showed that the radially graded porous receiver with a large pore diameter around the centre of the structure, matching the non-uniform solar radiation distribution reaching the receiver, outperforms non-radially graded porous receivers by distributing the air to high solar flux regions, reducing the surface temperature and thermal radiative loss.



(**a**) (**b**)

Figure 20. Optimisation of a radially graded porous volumetric receiver, as performed by Du et al. [14]: (**a**) 3D-printed two-layered sample (lower porosity in the inner layer; higher porosity in the outer layer), (**b**) multi-layer volumetric receiver parametrisation employed in the GA optimisation process. (Reprinted from [14] with permission from Elsevier).

Another attempt to optimise a gradually varied porous absorber/receiver was performed by [67] using a GA. In this study, Monte Carlo ray tracing was employed for calculating the distribution of the absorbed radiation, while the fluid flow, thermal radiation, and thermal convection phenomena were also evaluated. Integration of the aforementioned evaluations with a GA was then performed, and the objective was to find the optimal matching between the absorber/receiver porosity distribution (radial, axial, and bidirectional) (refer to Figure 21) and the non-uniform flux distribution at the inlet of the receiver.

A dimensionless evaluation criterion was set during optimisation, whose value yields high thermal efficiency and low flow resistance. It was shown that the method was able to find the optimal porosity distribution, achieving up to 9.76% higher thermal efficiency and 55.73% lower pressure drop when compared to a uniform porous absorber.

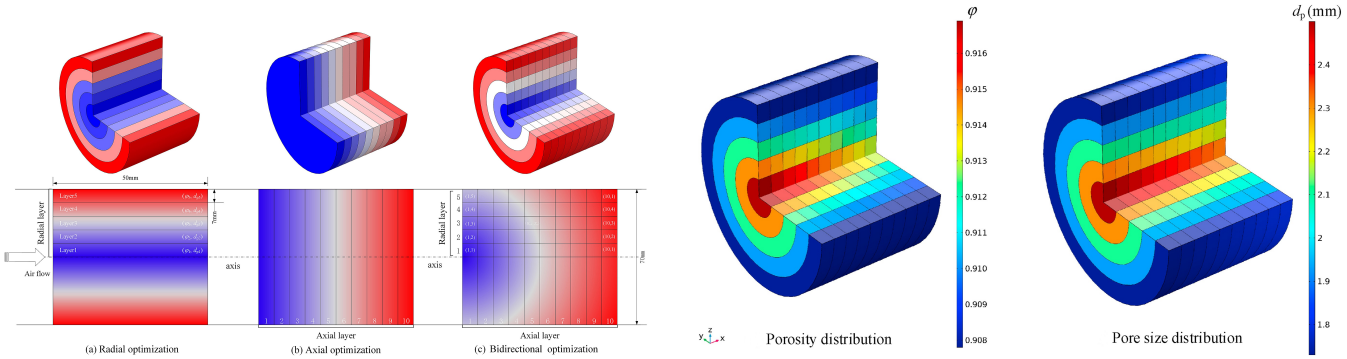


Figure 21. Optimisation of radial, axial, and bidirectional graded porous volumetric receivers, as performed by [67]: (**a**) radial, axial, and bidirectional parametrisation of the absorber/receiver geometry, (**b**) pore size distribution (left) and pore size distribution (right) of the bidirectional optimised absorber. (Reprinted from [67] with permission from Elsevier).

Finally, a deep neural network (DNN) technique was utilised in a study by Sharma and Talukdar [16], in which hydraulic, mechanical, and thermal analyses were considered during the evaluation and optimisation of a porous volumetric solar receiver. For training the DNN, numerical simulations were performed with various input parameters, including the porosity size of the foam, length, and the HTF inlet velocity, while as output, variables such as the pressure drop across the receiver and the outlet fluid temperature were selected. Later on within the study, the authors integrated the DNN with the NSGA-II algorithm to solve the multi-objective optimisation problem of finding receiver configurations that could prevent mechanical failure. During the optimisation process, the objective of NSGA-II was to search for the best receiver design given three objective functions, i.e., maximisation of the outlet fluid temperature, minimisation of the pressure drop, and a constraint that assures that the calculated stress remains below a maximum allowable stress. It is reported that the methodology is promising in terms of significantly reducing the computational time of the optimisation problem when compared to conventional approaches.

7. Discussion

Metaheuristic algorithms are typically employed in optimisation problems where the objective function is either unknown or impractical to solve analytically. Despite the existence of hundreds of metaheuristic algorithms Ma et al. [68], only a small fraction have been applied to solar tower receiver generative design. Among these, GA variations are the most commonly used, as depicted in Figure 22, being used in 60% of the studies included in this review. This prevalence is likely due to the fact that GAs were among the first developed metaheuristic algorithms. However, a wider range of metaheuristic algorithms has been implemented in solving optimisation problems for other solar thermal systems and/or components, as noted by Olabi et al. [17], Conroy et al. [69], Milidonis et al. [70], Vakili and Salehi [71], Elsheikh and Elaziz [72].

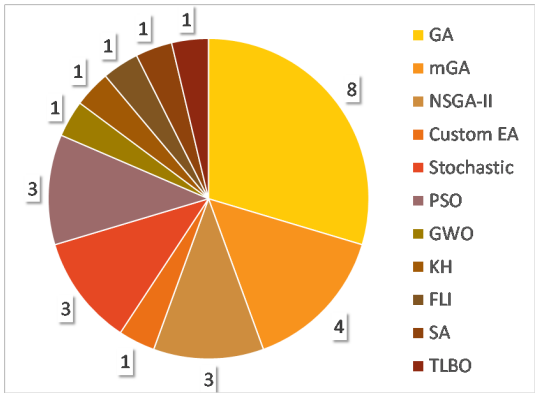


Figure 22. Pie chart of the metaheuristic algorithms used for the generative design of solar tower receivers and radiant enclosures.

The No Free Lunch (NFL) theorem introduced by Wolpert and Macready [73] states that no "black-box" algorithm consistently outperforms all others across all optimisation problems. To establish that one algorithm performs better than another on average, it must demonstrate superior performance across a sufficiently large sample of problems. Furthermore, the performance of the same algorithm can vary significantly depending on the hyperparameter settings. Under these premises, optimisation studies on cavity, external, and volumetric solar tower receivers differ substantially in nature, making direct comparisons inappropriate, as the problems being addressed are fundamentally different.

Another challenge is that the best-found solution cannot be guaranteed to be the global optimum, as the algorithm may converge to a local minimum. The primary approach to mitigate this issue involves tuning the algorithm's hyperparameters. In extreme cases, switching to a different metaheuristic algorithm may be necessary. Despite the widespread use of these algorithms, many studies fail to report key hyperparameters, such as population size, crossover and mutation probabilities, or decay factors. Incorporating problem-specific metrics that quantify the gap between the optimised solution and a theoretical or analytical global optimum would enhance the reliability of such studies. A clear example of the impact of hyperparameter selection can be found when comparing the studies of Sarvari [50] and Farahmand et al. [51]. In Sarvari [50], the use of an mGA with an extremely small population size of only five individuals likely caused the algorithm to become trapped in a local minimum, which was stated in the study as the optimal solution. Conversely, Farahmand et al. [51] obtained a better-performing solution for the same problem by employing a population size of 50 individuals, demonstrating the importance of properly selected hyperparameters. These studies on the geometry optimisation of similar radiant enclosures suggest that the mGA is not a suitable algorithm for this problem. The receiver design problem typically involves the optimisation of a relatively high number of parameters (often more than 10) within a large search space. Using a small population size increases the likelihood of the algorithm getting trapped in local minima. Escaping such minima requires more evaluations, and, with a low mutation rate, the algorithm may be unable to do so at all. Choosing an appropriate population size involves a trade-off between computational cost and convergence effectiveness. While larger populations demand greater computational effort per generation, they enhance individual diversity, reducing the risk of premature convergence. Homogeneous populations with insufficient mutation rates often lead to stagnation in local minima. Among the studies reviewed, the most effective population sizes range from 50 to 200 individuals when the number of optimisation variables is between 5 and 15. Both the PSO and KH algorithms have demonstrated better performance in radiant enclosure problems, being able to identify

global optima. A KH variation has also shown faster convergence than PSO, although further studies on hyperparameter tuning for PSO are still needed.

A summary of the different studies reviewed can be found in Table 1. While metaheuristic algorithms have proven to be powerful optimisation tools, some studies lack sufficient detail about the algorithm configurations. For instance, population size, which is a critical hyperparameter, is sometimes omitted, making it impossible to determine the total number of fitness evaluations required to reach an optimal solution.

Table 1. Review of metaheuristic algorithms employed in the literature.

Receiver Type	References	Method	Population Size	Decision Variables	Objectives
Cavity	[43,44]	Stoch. Opt.	1000	ND	Maximise power absorbed
Cavity	[42]	NSGA-II	ND	36	Maximise flux uniformity Minimise optical loss
Cavity	[60]	NSGA-II	12	9	Maximise thermal efficiency
Cavity	[47]	Custom EA	ND	9	Maximise annual thermal yield
Cavity	[48]	GA, SA, GWO, PSO	ND	11	Maximise efficiency
Radiant enclosure	[50]	mGA	6	6–12	Maximise flux uniformity
Radiant enclosure	[54,56,57]	mGA	5	1–30	Maximise flux uniformity
Radiant enclosure	[51]	PSO	20–40	6–14	Maximise flux uniformity
Radiant enclosure	[49]	GA	100	4	Maximise flux uniformity
Radiant enclosure	[52]	KH	50	1–7	Maximise flux uniformity
Radiant enclosure	[55]	TLBO	40	5–20	Maximise flux uniformity
External	[63]	Stoch. Opt.	10	10	Maximise work efficiency Minimise receiver area Minimise receiver temperature
External	[64]	GA	ND	7	Minimise LCOH
External	[62]	GA	1000	6	Maximise receiver lifetime
External	[61]	GA	50	5	Maximise thermal efficiency Minimise LCOE
Volumetric	[14,65,66]	GA	100	5	Maximise thermal efficiency
Volumetric	[67]	GA	ND	5–100	Maximise thermal efficiency Minimise flow resistance

ND: Not defined.

In addition, a complete and detailed problem definition is often missing. Although the number of decision variables is usually specified, the full span of the search space is frequently omitted. For example, in continuous optimisation, the number of possible solutions depends not only on the range limits but also on the resolution and the step size between adjacent possible values. Given the high computational cost of optical and thermal evaluations in solar tower receiver design, both the search space resolution and its documentation in the algorithm description are critical.

To mitigate the high computational cost of numerical tools, ANNs are chosen for accelerating the optimisation process, often achieving computational speedups of 500 to 1000 times. Most of the times ANNs are trained on data extracted from simulations following the parametrisation of the problem. A summary of the studies using ANNs for solar tower receivers can be found in Table 2. The correlation between the results provided by the trained ANNs and the simulation tools shows perfect agreement in every study, as the R^2 is always very close to 1. The ANN in [48] is also fine-tuned with experimental data, i.e., [48], enhancing its reliability as an alternative simulation tool while maintaining the advantage of performing fast evaluations.

Table 2. Review of MLP-ANNs employed in the literature.

Receiver Type	Reference	Loss Function	Inputs	Predictions	Epochs	R^2
Cavity	[45]	MSE	Sun irradiance Tube diameter Cavity depth	Collector efficiency	ND	0.99
Cavity	[46]	MRE / MSE	Diameter ratio Inclination angle Wall temperature Insulation thickness Emissivity Air density	Convective losses Radiative losses	ND	0.982
Cavity	[47]	MSE	Solar zenith angle Solar azimuth angle Absorbed solar radiation Ambient temperature Wind speed HTF outlet temperature	HTF pressure loss Power absorbed	1000	ND
Cavity	[48]	MSE	Aperture diameter Bottom diameter Cavity length Tube diameter Tube numbers Incident energy HTF inlet temperature HTF inlet flow rate Flux at 32 receiver surface elements	HTF outlet temperature Thermal efficiency Maximum temperature HTF pressure drop	1000	0.9989
Radiant enclosure	[59]	MSE	Heat power Design surface temperature Surface emissivity H_2O and CO_2 gas concentrations Heaters configurations	4 radiative fluxes	1000	0.999
Volumetric	[16]	Relative error	Porosity Pore size HTF inlet velocity Absorber length	HTF outlet temperature HTF pressure drop Failure index	ND	0.999

ND: Not defined.

However, the ANNs are highly inflexible and not generalisable, as their inputs and outputs are specifically tailored to the parametrised problem; thus, they are not applicable in other scenarios. Most studies employ mean squared error (MSE) as the primary loss function, a standard choice in AI applications due to its strong penalty on large prediction errors. Nonetheless, the training process is often underreported, with missing details on batch sizes, optimisers, data normalisation techniques, and how frequently gradients are computed (e.g., per epoch or per batch).

8. Conclusions

Solar tower thermal receiver design involves solving a complex, multi-variable optimisation problem using numerical approaches. Unlike traditional design processes guided by expert experience, metaheuristic algorithms have demonstrated superior efficiency in navigating complex optimisation landscapes. However, their application often involves evaluating a vast number of candidate designs, which leads to significantly higher computational costs. The increased computational cost is observed to be mitigated by the replacement of the simulation tools by trained ANNs.

This review has examined the use of both metaheuristic algorithms and ANNs in the generative design of solar tower receivers. Given the similarities between cavity receivers and radiant enclosures, the scope of this review also includes relevant studies on radiant enclosures. To the best of our knowledge, this is the first literature review that focuses specifically on the receiver component of solar thermal towers, excluding other CST plant

subsystems, while incorporating insights from radiant enclosure optimisation, which is widely studied in industrial heat treatment processes and maintains high similarity with cavity receivers.

Metaheuristic algorithms have been in use for several decades; as a result, their application in solar energy systems is more widespread, with 22 studies identified compared to only six involving ANNs. One of the key challenges observed across the literature is the definition of the search space, including the number of optimisation variables and the resolution of continuous variables. This aspect critically affects convergence behaviour and computational load. To manage this cost, many studies intentionally limit the number of variables, which ultimately constrains the level of detail and innovation of the resulting designs. Moreover, there exists a need to have benchmarked tests to properly compare existing and emerging receiver designs under the same conditions.

The adoption of ANNs has proven effective in reducing the cost of fitness evaluations during optimisation. However, a lack of standardisation across studies persists. Most research efforts rely on proprietary tools, non-public simulation environments, and unique design parametrisations. As each study generates its own training dataset, the resulting models are highly problem-specific and lack transferability. Establishing standardised design parametrisations and promoting open access to datasets, including experimental data, could enable the development and reuse of pre-trained models, thereby accelerating progress in CST technology.

Lowering the cost of performance evaluations also opens the door to more rigorous comparisons of algorithm performance and hyperparameter tuning. It is important to note that due to the stochastic nature of many metaheuristic algorithms, such as those involving mutation or parent selection, multiple independent runs are essential to obtain statistically reliable results.

In conclusion, this review highlights that AI-driven generative design methods, particularly those combining metaheuristics and ANNs, offer a promising pathway for accelerating the development of solar tower receivers. These approaches have already demonstrated the potential to outperform traditional design methods in terms of both efficiency and performance. Among the reviewed studies, the optimisation focus has largely been limited to the optical domain, primarily evaluated using Monte Carlo ray tracing.

Looking ahead, several promising research directions can enhance the role of AI in the generative design of CST tower receivers. A key opportunity lies in the integration of multi-physics simulation tools, such as computational fluid dynamics (CFD), ray tracing, and thermo-structural analysis, into AI-driven optimisation workflows, enabling more physically accurate and performance-oriented design outcomes. Additionally, the incorporation of experimental validation data into generative models remains largely unexplored and could significantly improve the accuracy, reliability, and generalisability of optimisation results. The development of standardised benchmark cases and open-access datasets would also support more systematic evaluation and comparison of algorithms across receiver types. Finally, emerging concepts such as uncertainty quantification and digital twin frameworks present exciting opportunities to extend generative design into more robust and adaptive paradigms, potentially enabling real-time design iteration and predictive optimisation in the future development of intelligent CST receiver systems.

Author Contributions: Conceptualization: K.M.; methodology K.M. and J.M.G.-M.; K.M. and J.M.G.-M.; software J.M.G.-M.; validation K.M. and J.M.G.-M.; formal analysis J.M.G.-M.; investigation J.M.G.-M.; resources K.M. and J.M.G.-M.; data curation J.M.G.-M.; writing—original draft preparation K.M. and J.M.G.-M.; writing—review and editing K.M. and J.M.G.-M.; visualization K.M. and J.M.G.-M.; supervision K.M.; project administration K.M.; funding acquisition K.M. All authors have read and agreed to the published version of the manuscript.

Funding: This study was funded by the European Union's Horizon 2020 research and innovation programme under the Marie Skłodowska-Curie grant agreement no 101072537.

Data Availability Statement: No new data were created or analysed in this study.

Conflicts of Interest: The authors declare no conflicts of interest.

References

1. McKnight, M. Generative Design: What it is? How is it being used? Why it's a game changer. *KnE Eng.* **2017**, *2*, 176–181. [CrossRef]
2. Regenwetter, L.; Nobari, A.H.; Ahmed, F. Deep Generative Models in Engineering Design: A Review. *J. Mech. Des.* **2022**, *144*, 071704. [CrossRef]
3. Chu, T.; Pei, Y.; Cheng, P. A Generative Design Method for Typical Structural Parts of Aircraft. *J. Phys. Conf. Ser.* **2023**, *2562*, 012073. [CrossRef]
4. Skarka, W.; Nalepa, R.; Musik, R. Integrated Aircraft Design System Based on Generative Modelling. *Aerospace* **2023**, *10*, 677. [CrossRef]
5. Chen, W.; Chiu, K.; Fuge, M. Aerodynamic Design Optimization and Shape Exploration using Generative Adversarial Networks. In Proceedings of the AIAA Scitech 2019 Forum, San Diego, CA, USA, 7–11 January 2019. [CrossRef]
6. Junk, S.; Rothe, N. Lightweight design of automotive components using generative design with fiber-reinforced additive manufacturing. *Procedia CIRP* **2022**, *109*, 119–124. [CrossRef]
7. Dilibal, C.; Davis, B.L.; Chakraborty, C. Generative Design Methodology for Internet of Medical Things (IoMT)-based Wearable Biomedical Devices. In Proceedings of the 2021 3rd International Congress on Human-Computer Interaction, Optimization and Robotic Applications (HORA), Ankara, Turkey, 11–13 June 2021; pp. 1–4. [CrossRef]
8. Mukkavaara, J.; Sandberg, M. Architectural Design Exploration Using Generative Design: Framework Development and Case Study of a Residential Block. *Buildings* **2020**, *10*, 201. [CrossRef]
9. Vahdatikhaki, F.; Salimzadeh, N.; Hammad, A. Optimization of PV modules layout on high-rise building skins using a BIM-based generative design approach. *Energy Build.* **2022**, *258*, 111787. [CrossRef]
10. Lukin, A.; Perepelkina, S.; Demidova, G.; Lukichev, D.; Rassõlkin, A.; Vaimann, T.; Kallaste, A. Generative Design in Development of Mechanical Components for Magnus Effect-Based Wind Turbine. In Proceedings of the 2020 XI International Conference on Electrical Power Drive Systems (ICEPDS), Saint-Petersburg, Russia, 4–7 October 2020; pp. 1–5. [CrossRef]
11. Santos, G.B.; Pantaleão, A.V.; Salviano, L.O. Using deep generative adversarial network to explore novel airfoil designs for vertical-axis wind turbines. *Energy Convers. Manag.* **2023**, *282*, 116849. [CrossRef]
12. Noone, C.J.; Torrilhon, M.; Mitsos, A. Heliostat field optimization: A new computationally efficient model and biomimetic layout. *Sol. Energy* **2012**, *86*, 792–803. [CrossRef]
13. Ballestrín, J.; Carra, E.; Alonso-Montesinos, J.; López, G.; Polo, J.; Marzo, A.; Fernández-Reche, J.; Barbero, J.; Batlles, F.J. Modeling solar extinction using artificial neural networks. Application to solar tower plants. *Energy* **2020**, *199*, 117432. [CrossRef]
14. Du, S.; Xia, T.; He, Y.L.; Li, Z.Y.; Li, D.; Xie, X.Q. Experiment and optimization study on the radial graded porous volumetric solar receiver matching non-uniform solar flux distribution. *Appl. Energy* **2020**, *275*, 115343. [CrossRef]
15. Ajbar, W.; Parrales, A.; Cruz-Jacobo, U.; Conde-Gutiérrez, R.A.; Bassam, A.; Jaramillo, O.A.; Hernández, J.A. The multivariable inverse artificial neural network combined with GA and PSO to improve the performance of solar parabolic trough collector. *Appl. Therm. Eng.* **2021**, *189*, 116651. [CrossRef]
16. Sharma, S.; Talukdar, P. Implementation of Deep Neural Networks for performance prediction and optimization of a porous volumetric solar receiver considering mechanical safety. *Appl. Therm. Eng.* **2023**, *232*, 121096. [CrossRef]
17. Olabi, A.G.; Abdelghafar, A.A.; Maghrabie, H.M.; Sayed, E.T.; Rezk, H.; Radi, M.A.; Obaideen, K.; Abdelkareem, M.A. Application of artificial intelligence for prediction, optimization, and control of thermal energy storage systems. *Therm. Sci. Eng. Prog.* **2023**, *39*, 101730. [CrossRef]
18. Wang, Y.; Wu, Z.; Ni, D. Real-Time Optimization of Heliostat Field Aiming Strategy via an Improved Swarm Intelligence Algorithm. *Appl. Sci.* **2024**, *14*, 416. [CrossRef]
19. Kabengele, K.T.; Olayode, I.O.; Tartibu, L.K. Analysis of the Performance of a Hybrid Thermal Power Plant Using Adaptive Neuro-Fuzzy Inference System (ANFIS)-Based Approaches. *Appl. Sci.* **2023**, *13*, 11874. [CrossRef]
20. Zaaoumi, A.; Bah, A.; Ciocan, M.; Sebastian, P.; Balan, M.C.; Mechaqrane, A.; Alaoui, M. Estimation of the energy production of a parabolic trough solar thermal power plant using analytical and artificial neural networks models. *Renew. Energy* **2021**, *170*, 620–638. [CrossRef]
21. Ouali, H.A.L.; Touili, S.; Merrouni, A.A.; Moukhtar, I. Artificial neural Network-Based LCOH estimation for concentrated solar power plants for industrial process heating applications. *Appl. Therm. Eng.* **2024**, *236*, 121810. [CrossRef]
22. Ho, C.K. Advances in central receivers for concentrating solar applications. *Sol. Energy* **2017**, *152*, 38–56. [CrossRef]

23. Madhlopa, A. *Solar Receivers for Thermal Power Generation Fundamentals and Advanced Concepts*; Academic Press: New York, NY, USA, 2022.
24. Rodríguez-Sánchez, M.R.; Soria-Verdugo, A.; Almendros-Ibáñez, J.A.; Acosta-Iborra, A.; Santana, D. Thermal design guidelines of solar power towers. *Appl. Therm. Eng.* **2014**, *63*, 428–438. [CrossRef]
25. Logie, W.R.; Pye, J.D.; Coventry, J. Thermoelastic stress in concentrating solar receiver tubes: A retrospect on stress analysis methodology, and comparison of salt and sodium. *Sol. Energy* **2018**, *160*, 368–379. [CrossRef]
26. Jiang, K.; Du, X.; Kong, Y.; Xu, C.; Ju, X. A comprehensive review on solid particle receivers of concentrated solar power. *Renew. Sustain. Energy Rev.* **2019**, *116*, 109463. [CrossRef]
27. Gentile, G.; Picotti, G.; Binotti, M.; Cholette, M.E.; Manzolini, G. A comprehensive methodology for the design of solar tower external receivers. *Renew. Sustain. Energy Rev.* **2024**, *193*, 114–153. [CrossRef]
28. Votyakov, E.V.; Papanicolas, C.N. Consistent multiphysics simulation of a central tower CSP plant as applied to ISTORE. *AIP Conf. Proc.* **2017**, *1850*, 160027. [CrossRef]
29. Požívil, P.; Ackermann, S.; Steinfeld, A. Numerical Heat Transfer Analysis of a 50 kWth Pressurized-Air Solar Receiver. *J. Sol. Energy Eng.* **2015**, *137*, 064504 . [CrossRef]
30. Ávila Marín, A.L. Volumetric receivers in Solar Thermal Power Plants with Central Receiver System technology: A review. *Sol. Energy* **2011**, *85*, 891–910. [CrossRef]
31. Holland, J. *Adaptation in Natural and Artificial Systems: An Introductory Analysis with Applications to Biology, Control, and Artificial Intelligence*; MIT Press: Cambridge, MA, USA, 1975; p. 211.
32. Krishnakumar, K. Micro-Genetic Algorithms For Stationary And Non-Stationary Function Optimization. In Proceedings of the Intelligent Control and Adaptive Systems, Philadelphia, PA, USA, 7–8 November 1989; Volume 1196, p. 289. [CrossRef]
33. Siinivas, N.; Deb, K. Muiltiobj ective Optimization Using Nondominated Sorting in Genetic Algorithms. *Evol. Comput.* **1994**, *2*, 221–248. [CrossRef]
34. Deb, K.; Pratap, A.; Agarwal, S.; Meyarivan, T. A fast and elitist multiobjective genetic algorithm: NSGA-II. *IEEE Trans. Evol. Comput.* **2002**, *6*, 182–197. [CrossRef]
35. Deb, K.; Jain, H. An evolutionary many-objective optimization algorithm using reference-point-based nondominated sorting approach, Part I: Solving problems with box constraints. *IEEE Trans. Evol. Comput.* **2014**, *18*, 577–601. [CrossRef]
36. Kennedy, J.; Eberhart, R. Particle Swarm Optimization. In Proceedings of the IEEE International Conference on Neural Networks, Perth, Australia, 27 November–1 December 1995; Volume 4, pp. 1942–1948. [CrossRef]
37. Gandomi, A.H.; Alavi, A.H. Krill herd: A new bio-inspired optimization algorithm. *Commun. Nonlinear Sci. Numer. Simul.* **2012**, *17*, 4831–4845. [CrossRef]
38. Mirjalili, S.; Mirjalili, S.M.; Lewis, A. Grey Wolf Optimizer. *Adv. Eng. Softw.* **2014**, *69*, 46–61. [CrossRef]
39. Rao, R.V.; Savsani, V.J.; Vakharia, D.P. Teaching-learning-based optimization: A novel method for constrained mechanical design optimization problems. *CAD Comput. Aided Des.* **2011**, *43*, 303–315. [CrossRef]
40. Rao, R.V.; Savsani, V.J.; Vakharia, D.P. Teaching-Learning-Based Optimization: An optimization method for continuous non-linear large scale problems. *Inf. Sci.* **2012**, *183*, 1–15. [CrossRef]
41. Kirkpatrick, S.; Gelatt, C.D.; Vecchi, M.P. Optimization by Simulated Annealing. *Science* **1983**, *220*, 671–680. [CrossRef]
42. Wang, K.; He, Y.L.; Li, P.; Li, M.J.; Tao, W.Q. Multi-objective optimization of the solar absorptivity distribution inside a cavity solar receiver for solar power towers. *Sol. Energy* **2017**, *158*, 247–258. [CrossRef]
43. Asselineau, C.A.; Zapata, J.; Pye, J. Integration of Monte-Carlo ray tracing with a stochastic optimisation method: Application to the design of solar receiver geometry. *Opt. Express* **2015**, *23*, A437. [CrossRef]
44. Asselineau, C.A.; Zapata, J.; Pye, J. Geometrical Shape Optimization of a Cavity Receiver Using Coupled Radiative and Hydrodynamic Modeling. *Energy Procedia* **2015**, *69*, 279–288. [CrossRef]
45. Loni, R.; Kasaeian, A.; Shahverdi, K.; Asli-Ardeh, E.A.; Ghobadian, B.; Ahmadi, M.H. ANN model to predict the performance of parabolic dish collector with tubular cavity receiver. *Mech. Ind.* **2017**, *18*, 408. [CrossRef]
46. Vikram, T.S.; Reddy, K.S. Investigation of convective and radiative heat losses from modified cavity based solar dish steam generator using ANN. *Int. J. Therm. Sci.* **2015**, *87*, 19–30. [CrossRef]
47. Schöttl, P.; Bern, G.; van Rooyen, D.W.; Pretel, J.A.F.; Fluri, T.; Nitz, P. Optimization of Solar Tower molten salt cavity receivers for maximum yield based on annual performance assessment. *Sol. Energy* **2020**, *199*, 278–294. [CrossRef]
48. Shuai, W.; Xu, H.; Luo, B.; Huang, Y.; Chen, D.; Zhu, P.; Xiao, G. Multi-objective optimizations of solar receiver based on deep learning strategy in different application scenarios. *Sol. Energy* **2024**, *267*, 112201. [CrossRef]
49. Darvishvand, L.; Kowsary, F.; Jafari, P.H. Optimization of 3-D radiant enclosures with the objective of uniform thermal conditions on 3-D design bodies. *Heat Transf. Eng.* **2016**, *37*, 1–12. [CrossRef]
50. Sarvari, S.M. Optimal geometry design of radiative enclosures using the genetic algorithm. *Numer. Heat Transf. Part A Appl.* **2007**, *52*, 127–143. [CrossRef]

51. Farahmand, A.; Payan, S.; Sarvari, S.M.H. Geometric optimization of radiative enclosures using PSO algorithm. *Int. J. Therm. Sci.* **2012**, *60*, 61–69. [CrossRef]
52. Sun, S.; Qi, H.; Zhao, F.; Ruan, L.; Li, B. Inverse geometry design of two-dimensional complex radiative enclosures using krill herd optimization algorithm. *Appl. Therm. Eng.* **2016**, *98*, 1104–1115. [CrossRef]
53. Sun, S.; Wang, G.; Chen, H. Application of decentralized fuzzy inference method for the inverse geometry design of radiative enclosures. *Infrared Phys. Technol.* **2020**, *107*, 103287. [CrossRef]
54. Amiri, H.; Mansouri, S.H.; Safavinejad, A.; Coelho, P.J. The optimal number and location of discrete radiant heaters in enclosures with the participating media using the micro genetic algorithm. *Numer. Heat Transf. Part A Appl.* **2011**, *60*, 461–483. [CrossRef]
55. Amiri, H.; Radfar, N.; Arab Solghar, A.; Mashayekhi, M. Two ımproved teaching—Learning-based optimization algorithms for the solution of ınverse boundary design problems. *Soft Comput.* **2023**, *27*, 12133–12154. [CrossRef]
56. Safavinejad, A.; Mansouri, S.H.; Sakurai, A.; Maruyama, S. Optimal number and location of heaters in 2-D radiant enclosures composed of specular and diffuse surfaces using micro-genetic algorithm. *Appl. Therm. Eng.* **2009**, *29*, 1075–1085. [CrossRef]
57. Amiri, H.; Coelho, P.J. A parametric study of optimal number and location of radiant heaters in enclosures with participating media. *Sci. Iran. B* **2016**, *23*, 206–217. [CrossRef]
58. Payan, S.; Farahmand, A.; Sarvari, S.M.H. Inverse boundary design radiation problem with radiative equilibrium in combustion enclosures with PSO algorithm. *Int. Commun. Heat Mass Transf.* **2015**, *68*, 150–157. [CrossRef]
59. Yadav, R.; Balaji, C.; Venkateshan, S.P. Optimization of number and locations of discrete heaters in a two-dimensional radiant heating furnace using artificial neural networks. *J. Energy Environ. Sustain.* **2019**, *8*, 12–18. [CrossRef]
60. Luo, L.; Du, W.; Wang, S.; Wang, L.; Sundén, B.; Zhang, X. Multi-objective optimization of a solar receiver considering both the dimple/protrusion depth and delta-winglet vortex generators. *Energy* **2017**, *137*, 1–19. [CrossRef]
61. Wang, S.; Asselineau, C.A.; Fontalvo, A.; Wang, Y.; Logie, W.; Pye, J.; Coventry, J. Co-optimisation of the heliostat field and receiver for concentrated solar power plants. *Appl. Energy* **2023**, *348*, 121513. [CrossRef]
62. Moreno, J.A.; Montoya, A.; López-Puente, J.; Santana, D. Lifetime optimization of solar central receivers via linear actuators. *Int. J. Mech. Sci.* **2022**, *226*, 107388. [CrossRef]
63. Asselineau, C.A.; Corsi, C.; Coventry, J.; Pye, J. Geometrical exploration of a flux-optimised sodium receiver through multi-objective optimisation. *AIP Conf. Proc.* **2017**, *1850*, 030002. [CrossRef]
64. Hussaini, Z.A.; King, P.; Sansom, C. Numerical simulation and design of multi-tower concentrated solar power fields. *Sustainability* **2020**, *12*, 2402. [CrossRef]
65. Du, S.; Ren, Q.; He, Y.L. Optical and radiative properties analysis and optimization study of the gradually-varied volumetric solar receiver. *Appl. Energy* **2017**, *207*, 27–35. [CrossRef]
66. Du, S.; He, Y.L.; Yang, W.W.; Liu, Z.B. Optimization method for the porous volumetric solar receiver coupling genetic algorithm and heat transfer analysis. *Int. J. Heat Mass Transf.* **2018**, *122*, 383–390. [CrossRef]
67. Li, J.B.; Wang, P.; Liu, D.Y. Optimization on the gradually varied pore structure distribution for the irradiated absorber. *Energy* **2022**, *240*, 122787. [CrossRef]
68. Ma, Z.; Wu, G.; Suganthan, P.N.; Song, A.; Luo, Q. Performance assessment and exhaustive listing of 500+ nature-inspired metaheuristic algorithms. *Swarm Evol. Comput.* **2023**, *77*, 101248. [CrossRef]
69. Conroy, T.; Collins, M.N.; Grimes, R. A review of steady-state thermal and mechanical modelling on tubular solar receivers. *Renew. Sustain. Energy Rev.* **2020**, *119*, 109591. [CrossRef]
70. Milidonis, K.; Blanco, M.J.; Grigoriev, V.; Panagiotou, C.F.; Bonanos, A.M.; Constantinou, M.; Pye, J.; Asselineau, C.A. Review of application of AI techniques to Solar Tower Systems. *Sol. Energy* **2021**, *224*, 500–515. [CrossRef]
71. Vakili, M.; Salehi, S.A. A review of recent developments in the application of machine learning in solar thermal collector modelling. *Environ. Sci. Pollut. Res.* **2023**, *30*, 2406–2439. [CrossRef]
72. Elsheikh, A.H.; Elaziz, M.A. Review on applications of particle swarm optimization in solar energy systems. *Int. J. Environ. Sci. Technol.* **2019**, *16*, 1159–1170. [CrossRef]
73. Wolpert, D.H.; Macready, W.G. No Free Lunch Theorems for Optimization. *IEEE Trans. Evol. Comput.* **2002**, *1*, 67–82. [CrossRef]

Disclaimer/Publisher's Note: The statements, opinions and data contained in all publications are solely those of the individual author(s) and contributor(s) and not of MDPI and/or the editor(s). MDPI and/or the editor(s) disclaim responsibility for any injury to people or property resulting from any ideas, methods, instructions or products referred to in the content.